REVIEW

National Science Review
4: 834–866, 2017
doi: 10.1093/nsr/nwx150

GEOSCIENCES

Special Topic: Air Pollution and Control

Anthropogenic emission inventories in China: a review

Meng Li[1,4,†], Huan Liu[2,†], Guannan Geng[1], Chaopeng Hong[1], Fei Liu[2], Yu Song[3], Dan Tong[1], Bo Zheng[2], Hongyang Cui[1], Hanyang Man[2], Qiang Zhang[1,*] and Kebin He[2,*]

[1]Ministry of Education Key Laboratory for Earth System Modeling, Department for Earth System Science, Tsinghua University, Beijing 100084, China; [2]State Key Joint Laboratory of Environment Simulation and Pollution Control, School of Environment, Tsinghua University, Beijing 100084, China; [3]State Key Joint Laboratory of Environmental Simulation and Pollution Control, Department of Environmental Science, Peking University, Beijing 100871, China and [4]now at Max-Planck Institute for Chemistry, Mainz, Germany

*Corresponding authors. E-mails: qiangzhang@tsinghua.edu.cn; hekb@tsinghua.edu.cn

†Equally contributed to this work.

Received 1 October 2017; Revised 4 December 2017; Accepted 24 December 2017

ABSTRACT

The development of reliable anthropogenic emission inventories is essential for both understanding the sources of air pollution and designing effective air-pollution-control measures in China. However, it is challenging to quantify emissions in China accurately, given the variety of contributing sources, the complexity of the technology mix and the lack of reliable measurements. Over the last two decades, tremendous efforts have been made to improve the accuracy of emission inventories, and significant improvements have been realized. More reliable statistics and survey-based data have been used to reduce the uncertainties in activity rates and technology distributions. Local emission factors and source profiles covering various sources have been measured and reported. Based on these local databases, improved emission inventory models have been developed for power plants, large industrial plants and the residential, transportation and agricultural sectors. In this paper, we review the progress that has been made in developing inventories of anthropogenic emissions in China. We first highlight the major updates that have been made to emission inventory models and the underlying data by source category. We then summarize the sector-based estimates of emissions of different species contained in current inventories. The progress that has been made in the development of model-ready emissions is also presented. Finally, we suggest future directions for further improving the accuracy of emission inventories in China.

Keywords: emission inventory, atmospheric chemistry, China, chemical transport model, air pollution

INTRODUCTION AND BACKGROUND

Understanding emissions in China is essential for studies of atmospheric chemistry and climate. Specifically, anthropogenic emissions from China cause severe haze events, which lead to adverse health impacts and reductions in visibility. Quantifying these emissions accurately is challenging, due to the variety of contributing sources, the complexity of the technology mix and the lack of reliable local measurements within China. Developing a reliable emission inventory with high accuracy is of great importance for designing air-pollution-control measures.

One of the main goals of developing emission inventories is to provide gridded emissions for use as inputs in atmospheric and climate models. Emission inventories have been developed in supporting of scientific research projects in which modelling activities are always accompanied by top-down validations. Examples include the Transport and Chemical Evolution over the Pacific (TRACE-P) [1], Intercontinental Chemical Transport Experiment-Phase B (INTEX-B) [2], MIX for MICS-Asia (Model Inter-Comparison Study for Asia) [3], Hemispheric Transport of Air Pollution (HTAP) [4] and Evaluating the Climate and Air Quality Impacts of Short-Lived Pollutants (ECLIPSE) emission inventories [5]. Emissions have also been estimated to support policy-making by stakeholders. Examples include the Greenhouse gas-Air pollution Interactions and Synergies (GAINS) inventory model and inventories used in policy evaluations [6–8].

Within the last two decades, tremendous efforts have been made to develop reliable emission

© The Author(s) 2017. Published by Oxford University Press on behalf of China Science Publishing & Media Ltd. This is an Open Access article distributed under the terms of the Creative Commons Attribution License (http://creativecommons.org/licenses/by/4.0/), which permits unrestricted reuse, distribution, and reproduction in any medium, provided the original work is properly cited.

Downloaded from https://academic.oup.com/nsr/article-abstract/4/6/834/4775139
by guest
on 14 February 2018

inventories in China, and significant improvements have been made. Early emission inventories over China were conducted mainly using 'bottom-up' methodologies, which employ activity rates and emission factors (EFs); the values of these parameters were drawn from those determined for Western countries, due to the lack of local data [1,9–12]. To support the INTEX-B (Intercontinental Chemical Transport Experiment-Phase B) mission, Zhang *et al.* [2] used an improved, detailed technology-based approach to estimate emissions in China. Using a consistent inventory framework, Ohara *et al.* [12] developed the first emission inventory covering China (the Regional Emission inventory in Asia, REAS) that includes both the historical period and projections; this inventory was updated to REAS v2 by Kurokawa *et al.* [13]. Increasing numbers of emission inventories have been compiled by parameterizing up-to-date technology distributions, datasets containing local measurements and improved methodologies for specific source categories (e.g. [14–20]) or specified regions (e.g. [21–24]).

Reliable data are crucial in improving the accuracy of emission estimates. The government of China releases an annual statistical yearbook on energy consumption and product yields covering diverse source categories, and these data constitute the basic database of activity rates used in compiling inventories. Large emission gaps are found when different official statistics are used [25,26]. Quantifying and further reducing the uncertainties due to statistical data are presently focuses of study. Given the increasing numbers of detailed surveys and data-collection activities that are being conducted by the Ministry of Environmental Protection (MEP) of China, industrial associations and research groups, emission estimates at the level of individual units or production lines are becoming feasible.

Large numbers of real-world EFs have been measured in China. Chinese researchers have produced large quantities of local measurements for stationary, mobile and fugitive sources over the past two decades. These data significantly improve our understanding of emission characteristics in China. Surveys of technological evolution and the control measures that have been implemented are important in determining net EFs. Although these surveys are being conducted in increasing numbers, they are limited to specific sources, such as power plants, large industrial plants and vehicles. The evolution of technology-based EFs calculated in inventory models provides a basis for analyses of historical trends and projections of future emissions.

Tsinghua University has developed a uniform emission model framework, the Multi-resolution Emission Inventory for China (MEIC), to estimate anthropogenic emissions over China. The MEIC model is based on a series of improved emission inventory models including unit-based emission inventories for power plants [19] and cement plants [15]; a high-resolution county-level vehicle emission inventory [16]; a residential combustion emission inventory based on national-wide survey data [27]; and an explicit profile-based non-methane volatile organic compound (NMVOC) speciation framework [28]. MEIC provides the community a publically accessible emission dataset over China with regular updates (http://www.meicmodel.org).

Nine chemical species, including both gaseous and aerosol species, are included in this review, as they are always included as inputs to chemical transport models: SO_2 (sulphur dioxide), NO_x (nitrogen oxides), CO (carbon monoxide), NMVOCs, NH_3 (ammonia), PM_{10} (particulate matter with diameter less than or equal to 10 μm), $PM_{2.5}$ (particulate matter with diameter less than or equal to 2.5 μm), BC (black carbon) and OC (organic carbon). To fill the gap between the inventoried and modelled species, explicit speciation of the NMVOCs and PM (particulate matter) is required.

In this article, we review the considerable progress that has been made in the methods and data used in the estimation of emissions and the results of these estimates (second and third sections) and model-ready emissions processing (fourth section) in China. Main uncertainties in current inventories are discussed in the fifth section. Outlook for developing improved emission inventories over China are provided in the sixth section.

EMISSIONS BY SECTORS

In this section, we provide an overview of the development of emission inventories by sector and subsector that focuses on (i) the history of emission estimates, the challenges, and up-to-date methods used in estimating emissions; (ii) key data sources of activity rates, locally measured EFs and other significantly improved parameters; and (iii) emission estimates and trends for specific sectors. Sectoral emissions by pollutant for 2010 are summarized in Table 1 (derived from version 1.2 of MEIC).

Power plants

Power plants are major contributors to the total emissions of air pollutants in China, and they have been widely considered to be a separate sector in many emission inventories. As the largest consumer of coal in China, the power plant sector has reported its total fuel consumption in each province in the

Downloaded from https://academic.oup.com/nsr/article-abstract/4/6/834/4775139
by guest
on 14 February 2018

Table 1. Emission estimates by sectors in China, 2010 (derived from MEIC v1.2, www.meicmodel.org) (unit: Gg/year for the sectoral emissions, Tg/year for the total emissions).

Species	Power	Industry	Residential	Transportation	Solvent use	Agriculture	Total
SO_2	7779.06	16 372.99	4153.77	222.98			28.53
NO_x	9265.93	9344.26	1726.82	6982.79			27.32
CO	3632.28	74 739.76	71 281.77	20 323.67			169.98
NMVOCs	66.39	7878.63	5014.79	2351.98	7151.05		22.46
NH_3	0.00	273.57	427.65	25.42		9701.62	10.43
PM_{10}	978.19	6060.13	8068.53	497.78			15.60
$PM_{2.5}$	847.27	5805.25	4452.15	493.31			11.60
BC	1.75	584.35	848.19	273.13			1.71
OC	0.02	578.64	2481.50	99.61			3.16

official statistical yearbooks for over two decades (China Energy Statistical Yearbook, National Bureau of Statistics (NBS), 1992–2016). Early studies employed the reported annual fuel consumption values and fixed EFs to calculate the yearly emissions; however, this procedure does not accurately represent the rapid changes in emission rates driven by technological improvements [9,12,29,30]. Recent studies have adopted dynamic EFs derived from technology-based methodologies and locally measured EFs to improve the accuracy of both the magnitudes of power plant emissions and the trends in these emissions [1,2,31–35].

In addition to accurate estimates of total emissions, the spatial allocation of emissions is also important in power plant inventories for model applications and analyses. Ideally, emissions are estimated for individual power plants and allocated to grid cells using their exact geographical coordinates. However, due to the lack of detailed information (i.e. location, fuel consumption and emissions) on the power plants in China, many bottom-up inventories rely on a downscaling approach to estimate the spatial distribution of emissions. This approach ignores the differences in technology used at power plants; thus, different inventories indicate different unit-based emission rates. The early inventories only included information on large electricity-generating units and treat the remaining small units as area sources [1,12]. The emissions from large units were derived by downscaling provincial total emissions based on unit size [2,36]. Subsequent studies used a global power plant database, CARbon Monitoring for Action (CARMA) [37], which provides more extensive information (including the magnitudes of CO_2 emissions and locations) for individual power plants including small units, and breaks down the total emissions to the level of individual power plants [13,38,39]. The calculation of power plant emissions based on their unit-level coal consumption, instead of the downscaling approach, was initially performed by Zhao *et al.* [40] for 2000 and 2005 and allocated to the corresponding geographic coordinates. Similar unit-based power plant emission inventories were subsequently constructed for other years, including the period of 2005–07 (including only NO_x; [41]), the year 2010 (including only NO_x; [42]) and the year 2011 [43]. More recently, a unit-based power plant database that covers the period of 1990–2010, the China coal-fired Power plant Emissions Database (CPED), was developed; this database includes time-dependent information on the technologies, fuel consumption, EFs and locations of individual units [19]. This inventory was the first long-term, unit-based inventory to be constructed, and it permits improved estimates of the spatial distribution of emissions and their trends.

EFs change over time with the operation of new combustion or emission control technologies required by new emission standards and the changes in fuel property. The sulphur content of coal varies widely among power plants, and the national average value from 1990 to 2010 is 1.07–0.95% [19]. The sulphur retention ratios range from 0.10 [40] to 0.15 [2,19,44]. Flue-gas desulphurization (FGD) systems have been gradually installed to remove SO_2 emissions since 2005; the penetration of this technology has increased from 12% in 2005 to 86% in 2010. Because the operating conditions of installed FGD facilities improved after 2008 [45–47], the SO_2 removal efficiency improved accordingly, and a coal consumption weighted mean of 78% was reached for all FGD facilities in 2010 [19]. SO_2 emissions can also be removed from wet scrubbers as a co-benefit of PM removal and the corresponding suggested removal efficiency is 20% [48,49].

Table 2 summarizes the measured NO_x EFs for coal-fired power plants in China. The NO_x EFs are determined by boiler size, combustion technology and coal type. Low-NO_x burners (LNBs) were the only technology that was widely used to control NO_x emissions before 2010. Most power plants were

Downloaded from https://academic.oup.com/nsr/article-abstract/4/6/834/4775139
by guest
on 14 February 2018

Table 2. Summary of NO_x emission factors for different types of coal-fired power plants.

Unit size	Combustion technology	Bituminous coal, g/kg[a]	Anthracite coal, g/kg[a]
Large (≥300 MW)	Advanced LNB[b]	2.88[1], 3.05[2], 3.28[3], 3.55[4], 4.13[5], 4.17[6], 4.64[7]	6.14[7], 6.58[4], 6.99[8]
	Traditional LNB	4.40[9], 4.98[10], 5.23[11], 5.06[12], 5.65[8], 7.78[4]	4.61[11], 4.99[12], 7.77[7], 7.94[8], 8.05[10], 8.73[9]
Medium (≥100 MW and <300 MW)	Traditional LNB	4.34[10], 5.52[11], 6.97[13]	7.07[11], 7.56[10]
	Non-LNB	5.46[14], 8.12[11]	8.25[10], 12.11[11]
Small (<100 MW)	Non-LNB	6.55[15], 6.88[11]	10.01[15], 11.50[11]

[a]Sample weighted mean. [b]LNB: Low-NO_x burners. Data sources: [1]Qian [53]. [2]Cao and Liu [54]. [3]Zhu [55]. [4]Wang *et al.* [56]. [5]Yi *et al.* [57]. [6]Zhu *et al.* [58]. [7]Xie *et al.* [59]. [8]Wang *et al.* [60]. [9]Bi and Chen [61]. [10]Tian [62]. [11]Zhu [63]. [12]Zhu *et al.* [64]. [13]Feng and Yan [65]. [14]Zhao *et al.* [66]. [15]Zhao *et al.* [14].

Table 3. Summary of the mass fractions of particulate matter of different size fractions to the total particulate matter in fly ash for different types of boilers.

	Boiler type		
Size fraction	Pulverized boilers	Circulating fluidized beds	Grate furnaces
$PM_{>10}$	0.56[1], 0.61[2], 0.82[3], 0.82[4]	0.71[5]	0.72[4], 0.638[5]
$PM_{2.5–10}$	0.28[1], 0.37[2], 0.15[3], 0.13[4]	0.22[5]	0.18[4], 0.23[5]
$PM_{2.5}$	0.16[1], 0.02[2], 0.03[3], 0.05[4]	0.07[5]	0.10[4], 0.14[5]

Data sources: [1]Huang *et al.* [67]. [2]Liu *et al.* [68]. [3]Yi *et al.* [57]. [4]Zhao *et al.* [14]; in-field measurements. [5]Klimont *et al.* [51]; literature review.

required to be equipped with LNBs to meet emission standards [50]. Selective catalytic reduction (SCR) and selective non-catalytic reduction (SNCR) systems were subsequently employed, and their penetration increased from 13% in 2010 to nearly 90% in 2015.

PM emission rates are related to boiler types. Different types of boilers (pulverized coal boilers, circulating fluidized beds and grate furnaces) retain different fractions of ash (20%, 44% and 85%, respectively), and the corresponding PM size distributions are listed in Table 3 [51,52]. Cyclones, wet scrubbers, electrostatic precipitators and bag filters are widely used in power plants to remove PM, and the removal efficiencies of these technologies have been summarized by Lei *et al.* [34]. In addition, wet FGD systems can remove PM as a co-benefit of SO_2 removal.

Driven by the ever-increasing demand for electricity, power plant emissions have increased sharply since 1990. However, emissions have grown at significantly lower rates than electricity generation, given the technological changes that have occurred in the power sector. Figure 1 compares multi-year estimates for power plant emissions derived from bottom-up inventories that are available for multiple species and are widely used in the research community. Nearly all of the inventories reflect consistent trends for SO_2 emissions, which peaked in approximately 2006 owing to the installation of FGD systems. The SO_2 emission trends after 2005 in the Emission Database for Global Atmospheric Research (EDGAR) 4.2 differ from those of the other inventories, most likely due to a lack of information on the progress that has been made in controlling SO_2 emissions in power plants in China. In addition, the official estimates of SO_2 emissions published by the MEP (China Statistical Yearbook, NBS, 1997–2011) are generally lower than those reached by other studies. The NO_x emission trends display good consistency among all of the inventories. More recent NO_x estimates [19] are lower than the previous values [13,32], due to the smaller EFs adopted. The PM emission trends generally agree well with each other, except for REAS v2, which makes different assumptions regarding the penetration of PM removal devices.

Industry

Industry is the largest contributor of emissions of SO_2 (57%), NO_x (34%), CO (44%), NMVOCs (35%) and $PM_{2.5}$ (50%), and contributes over 34% of the total emissions of PM_{10} and BC in China (see Table 1 for 2010). These pollutants are emitted both from stationary industrial factories and by industrial processes. Cement plants, iron and steel plants and industrial boilers are identified as major contributors of SO_2, NO_x and PM. In recent years, unit-based emission inventories have been developed

Downloaded from https://academic.oup.com/nsr/article-abstract/4/6/834/4775139
by guest
on 14 February 2018

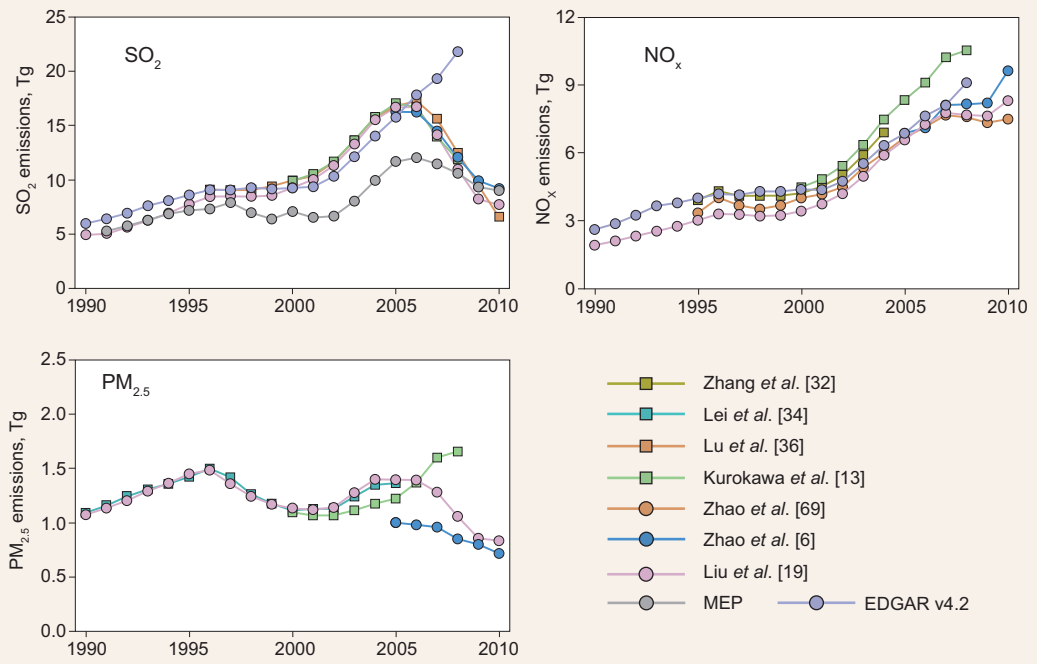

Figure 1. Comparisons of SO_2, NO_x and $PM_{2.5}$ emissions from China's coal-fired power plants during 1990 and 2010.

for cement plants [70] and iron and steel plants [71,72] based on detailed (factory-level) local information, which has substantially improved the development of emission estimates. The petroleum industry is the largest contributor to industrial emissions of NMVOCs, but these emissions are far from accurately quantified. We illustrate the emission estimates for the above subsectors separately below.

Cement

China is the largest producer and consumer of cement in the world. In 2014, cement production in China was as high as 2.49 billion metric tons, and this amount accounted for ~60% of the world's production [73]. The cement industry has been identified as one of the major contributors to the total national emissions of air pollutants in China. Several early studies treated the cement industry as a part of the industrial sector and estimated the corresponding emissions based on total coal consumption [1,12]. In addition, other studies applied uniform EFs to the reported cement production figures [74], and this practice did not reflect changes in technology and equipment replacement over time. Recent studies have developed dynamic EFs using technology-based methodologies [13,15,70,75,76] and local measurements have been incorporated, thus improving the accuracy of estimated emissions in China (e.g. [70,75,76]).

With the improvement of total estimated emission accuracy in the cement industry, the resolution of spatial distribution also has been improved gradually. Early studies adopted various spatial proxies to allocate total emissions to grid cells, due to the lack of detailed information for each cement plant (e.g. [1,75,77]). Recent studies allocate country and regional emissions using surrogate data developed based on the locations and annual capacities of the plants in each country and region (e.g. [13,15]). More recently, detailed plant-based information on large cement plants was collected and used to calculate plant-level emissions for the period of 1980–2012, and the remaining emissions were all treated as regional area sources in each province. This procedure significantly improves the accuracy of the inferred spatial distribution [70].

EFs reflect changes in technology over time. In general, two major types of kilns—shaft kilns and rotary kilns—are used in China. Due to the large emissions from shaft kilns, the use of precalciner kilns (the most advanced rotary kilns) has been promoted since the end of the 1990s. Therefore, equipment updates in cement plants in China have caused significant changes in the net EF.

The burning of fuel in the cement industry is usually identified as the sole source of SO_2 and NO_x emissions [15]. SO_2 is primarily produced by the oxidation of sulphur in fuels such as coal. In precalciner kilns, approximately 70% of SO_2 is absorbed by reaction with calcium oxide or calcium carbide [78], while much less is absorbed in other rotary kilns and in shaft kilns. Recent studies adopt the assumption that 80% of SO_2 is absorbed for

Downloaded from https://academic.oup.com/nsr/article-abstract/4/6/834/4775139
by guest
on 14 February 2018

Table 4. Summary of NO_x emission factors for different kiln types in cement industry.

Cement kiln types	NO_x emission factors (g/kg-clinker)[a, b]
Precalciner kilns	1.168[1], 1.535[2], 1.584[3,4,c], 1.494[5], 1.693[6], 1.746[3,d], 1.834[7], 2.016[8], 2.146[9]
Shaft kilns	0.202[3,e], 0.243[3,f], 0.482[10]
Other rotary kilns	1.609[1], 2.448[8]

[a]Sample weighted mean. [b]Assumptions introduced when transferring measurements to emission factor unit in g/kg-clinker: flue-gas volume is 2.47 m^3/kg-clinker (Wu [79]); average clinker to cement ratio is 0.72 (Lei *et al.* [15]); average coal consumption is 183g-coal/kg-clinker for precalciner and other rotary kilns, and 177g-coal/kg-clinker for shaft kilns (Zhang *et al.* [75]). [c]For precalciner kiln capacity ≥4000 t/d. [d]For precalciner kiln capacity <4000 t/d. [e]For shaft kiln capacity <10 0000 t/yr. [f]For shaft kiln capacity ≥10 0000 t/yr. Data sources: [1]Yuan *et al.* [80]. [2]Ren *et al.* [81]. [3]Handbook of Industrial Pollution Emission Factors. [4]Guo *et al.* [82]. [5]Liu *et al.* [83]. [6]Chen *et al.* [84]. [7]Wu *et al.* [79]. [8]Su *et al.* [85]. [9]Ding *et al.* [86]. [10]Li [87].

Table 5. Summary of the mass fractions of particulate matter of different size fractions to the total particulate matter in fly ash for different types of kilns.

	Kiln types		
Size fraction	Precalciner kilns	Shaft kilns	Other rotary kilns
$PM_{>10}$	0.18[1]	0.14[1]	0.11[1]
$PM_{2.5-10}$	0.24[1]	0.22[1]	0.20[1]
$PM_{2.5}$	0.58[1]	0.64[1]	0.69[1]

Data sources: [1]Lei *et al.* [76].

precalciner kilns, whereas this proportion is 30% for other kiln types. In general, SO_2 emissions are estimated using a mass balance approach and are based on the average sulphur content of coal in each province [15,70].

The generation of NO_x is highly influenced by kiln temperature and oxygen availability. Compared to shaft kilns, rotary kilns produce much more NO_x because of their higher operation temperatures and stable ventilation [15]. Table 4 summarizes the measured NO_x EFs in cement plants in China published in various studies. As awareness of the increasing NO_x emissions from the cement industry in China has grown, increasing numbers of SCR and SNCR systems have been requested for installation in the cement industry [70]. De-NO_x systems are reported to have been subsequently installed in precalciner kilns, and their penetration rate had reached nearly 92% as of 2015 (China's Ministry Environmental Protection).

Besides kilns, PM is emitted from several other emission sources, including quarrying and crushing, grinding and blending, packaging and loading, and the storage of raw material [15]. The PM EF depends on both the characteristics of unabated emissions from the overall production process and the removal efficiencies of PM emission control devices. As shown in Table 5, the three types of kilns emit PM with different size fraction distributions. PM control devices can reduce PM emissions by 10–99.9%, depending on the type of control technology employed and the size distribution of PM in the raw flue gas [76]. The removal efficiencies of various PM emission control devices are summarized by Lei *et al.* [15].

Large increases in cement production in China since 1980 have resulted in dramatic increases in emissions of air pollutants. Figure 2 compares multi-year estimates for cement plant emissions from bottom-up inventories that have been published by different researchers. The inventories developed by Lei *et al.* [15] and Hua *et al.* [70] provided comparatively consistent trends for SO_2, NO_x and PM emissions. These two studies show that SO_2 emissions increased rapidly from 1990 to 2003 and fell significantly after 2007. However, the peak SO_2 emissions estimated by Lei *et al.* [15] and Hua *et al.* [70] occurred in 2007 and 2003, respectively. A detailed comparison of the methods and data used in these two studies indicates that the differences in the trends in SO_2 emissions from 2003 to 2007 can be attributed to the derived province-level coal consumption. NO_x emissions show significant increases since 1980; emissions of this pollutant increased much faster than any other pollutant, due to the rapid expansion of precalciner kilns in China. These two studies display similar trends in PM emissions from 1990 to 2008. The emissions of PM rose rapidly from 1990 to 1995, and PM emissions decreased gradually, due to the replacement of shaft kilns by precalciner kilns and the application of high-performance PM removal technology, especially after 2004.

Iron and steel

China has been the largest producer and consumer of iron and steel in the world since 1996, to meet the rapidly growing demand of infrastructure construction. As an energy-intensive and pollution-intensive sector, it is estimated that the production of iron

Downloaded from https://academic.oup.com/nsr/article-abstract/4/6/834/4775139
by guest
on 14 February 2018

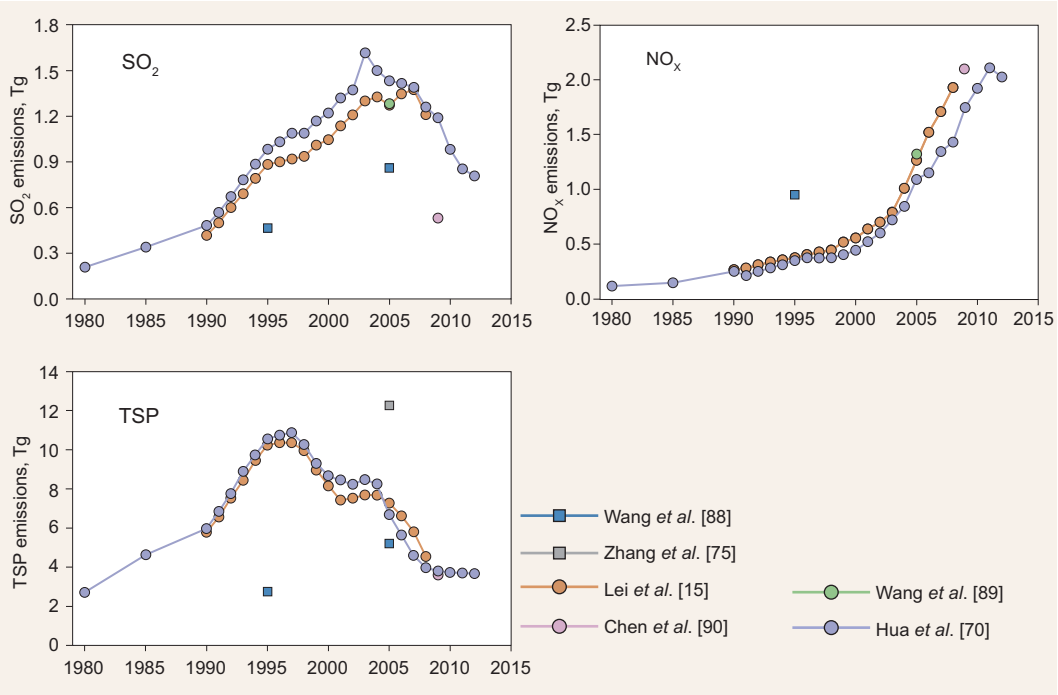

Figure 2. Comparisons of SO_2, NO_x and TSP emissions from China's cement industry during 1980 and 2012.

and steel contributed approximately 27% of the dust emissions, 20% of the SO_2 emissions and 8% of the NO_x emissions from all of the key manufacturing industries in China in 2013 [71]. The primary emissions characteristics of iron and steel production have been estimated by recent studies [71,72,91]. Wang *et al.* [71] proposed a unit-based bottom-up methodology that employs detailed information on 300 integrated steel plants in China, including steel production, capacity, geographical location and installation status of FGD systems. To accurately estimate the PM emissions, Wang *et al.* [71] developed an emission inventory model for the iron and steel industry that provided information on each emission node within the production process, including both stationary and fugitive sources. Activity rates, including the product yields for each process, are accessible from the official statistics (China Steel Yearbook, Steel Statistical Yearbook), the reports of the China Iron and Steel Industry Association and local literature.

The EFs of iron and steel production processes used in current emission inventories are mainly based on the Manual of Emission Coefficients, which was produced using industry census data from China and was released by the MEP in 2011. Western data and reports are available in corresponding publications, specifically the US EPA (Environmental Protection Agency)'s Compilation of Air Pollution Emission Factors (AP-42), the European Environment Agency (EEA) guidebook, the Best Available Techniques Reference Document for Iron and Steel Production released by the European Commission (EU-BAT) and the National Atmospheric Emissions Inventory for the UK (NAEI). The detailed EFs for different source categories can be found in the inventory papers [71,72].

End-of-pipe technologies for the control of SO_2 and PM with high removal efficiencies have been increasingly installed in iron and steel plants. By 2012, the proportion of wet FGD systems used in sintering reached 73.1% [91]. According to Wang *et al.* [72], the EFs for $PM_{2.5}$ decreased by 21.2% from 2006 to 2012, due to the implementation of emission control policies. The gas-recycling ratio in iron and steel plants reached values exceeding 96% in 2013 (as estimated by Wang *et al.* [71]). The government of China has released emission standards for the iron and steel industry (GB 28662–2012, GB 28663–2012, GB 28664–2012) and has provided instructions to adjust the industrial structure, which has also affected the net EFs.

Driven by the huge growth in production, the emissions of SO_2, NO_x and $PM_{2.5}$ due to the production of iron and steel increased from 1.22 to 2.31 Tg (+89%), 0.33 to 0.69 Tg (+97%) and 0.89 to 1.71 Tg (+92%), respectively, between 2005 and 2011 [71]. The emissions of PM began to decrease in 2012, due to the increasing control level. Sintering is the process that produces the largest amounts of all of these pollutants.

Downloaded from https://academic.oup.com/nsr/article-abstract/4/6/834/4775139
by guest
on 14 February 2018

Table 6. Summary of emission factors for industrial boilers[a].

Fuel type	SO_2	NO_x	CO	PM_{10}	$PM_{2.5}$	BC	OC
Briquette	19.9[1], 9.95[2,b]	1.63[2,b]	14[1], 11[2,b]	2.51[1], 0.24[3]	0.79[1], 0.219[2,b], 0.22[3]	0.0106[2,b]	0.0196[2,b]
Raw coal/bituminous	5.8[2], 5.65[2], 1.35[2], 2.9[2], 46.7[1]	1.71[2], 2.13[2], 2.38[2], 2.47[2]	1.43[2], 2.87[2], 9.05[2], 0.67[2], 15[1]	1.68[1], 0.13–0.65[3], 0.016[4], 0.1[4], 0.045[4]	0.209[2], 0.486[2], 0.059[2], 0.046[2], 0.87[1], 0.08–0.49[3], 1.14[3,c]	0.037[2], 0.018[2], 0.0013[2], 0.0014[2], 0.000062[4], 0.0028[4], 0.0007[4]	0.029[2], 0.026[2], 0.003[2], 0.006[2], 0.0003[4], 0.0171[4], 0.0019[4]

[a]Fuels are burned in grate boiler if not specified, unit: g/kg-fuel. [b]No control facilities. [c]Circulating fluidized beds. Data sources: [1]Ge *et al.* [92]. [2]Wang *et al.* [95]. [3]Li *et al.* [94]. [4]Zhang *et al.* [93].

Industrial boilers

Industrial boilers are important sources of emissions in China for NO_x, SO_2 and PM. In 2010, they released approximately 5.2 Tg of NO_x (20% of total emissions), 11.0 Tg of SO_2 (40%) and 0.96 Tg of $PM_{2.5}$ (8%) (estimated by MEIC v1.2). Of the industrial boilers in China, 85% are coal-fuelled. Approximately 50% of coal is burned in boilers with small capacities of $\leq$35 t/h that feature low combustion efficiencies and inefficient particulate emission control measures and desulphurization devices. Most industrial boilers in China are grate boilers, and small coal-fired boilers are especially prevalent. Cyclone or wet dust collectors are usually installed for PM abatement.

The EFs of coal combustion in industrial boilers have been reported by several native studies and are summarized in Table 6 [92–95]. PM components, including BC (EC in the original paper) and OC, have also been measured by Wang *et al.* [95] and Zhang *et al.* [93]. The measured EFs reported by different studies show very large differences, indicating substantial underlying uncertainties. Other key parameters that introduce uncertainties in emission estimates, including activity rates, fuel quality and technology distributions, are rarely investigated for industrial boilers in China. The development of a reliable local-scale database of industrial boilers in China is quite urgent.

To reduce the emissions, MEP of China released the emission standards for industrial boilers in 1983, and updated in 1991, 1999 and 2014 (GB 13271–2014). In the up-to-date emission standards, emission limits for SO_2 and NO_x are included that are separate from those of PM. However, little information on the effects of these environmental standards at the national level is available. Effective control measures have produced significant reductions in the emissions from industrial boilers in the megacities, such as Beijing and Shanghai. In Beijing, small scattered boilers have been shut down, highly efficient units have been constructed and the energy sources used have shifted from coal to cleaner fuels since 1998. As a result, reductions in the emissions from industrial boilers of 136 Gg of SO_2, 48.7 Gg of NO_x, 24 Gg of PM_{10} and 14.3 Gg of $PM_{2.5}$ were achieved between 1998 and 2013 [96]. Similar energy-saving measures have been carried out in Shanghai [97]. Other pioneering provinces, including Shandong, Heibei and Guangdong, have also released regional emission standards for industrial boilers, and the effects of implementing these standards have yet to be investigated and evaluated.

Petroleum industry

Petroleum-related industries are the largest contributors to industrial NMVOCs. These emissions are estimated based on the 'EF method' and are mainly produced by the exploitation, storage and transport of oil and gas, oil refineries, gas stations, the chemical industry and carbon black production. Qiu *et al.* [98] established a new classification of industrial sectors using a source-tracing method, which covers the emission sources in entire industries by tracing the material flow of NMVOCs in each industrial process. The industrial sources are grouped into four categories, which are the production of NMVOCs, the storage and transport of NMVOCs, industrial processes that use NMVOCs as raw materials and processes that use NMVOCs-containing products. This classification system was followed by Wu *et al.* [99] to characterize industrial emissions in China.

Local measurements of EFs for processes used in the petroleum industry are quite limited. Wei *et al.* [100] and Bo *et al.* [101] summarized the EFs of NMVOCs for the exploitation and distribution of oil and gas and oil refineries derived from reports from Western countries, including the US AP-42 database, the EEA guidebook and local emission standards. The EFs of rubber products were measured by Wu *et al.* [102]. A national standard (GB 11085–89) has been released for the storage and distribution of fossil fuels that provides a reference that can be used to determine the corresponding EFs.

Downloaded from https://academic.oup.com/nsr/article-abstract/4/6/834/4775139
by guest
on 14 February 2018

Residential

The residential consumption of fossil fuels (i.e. coal, oil and gas) for energy and biofuels (i.e. wood and crop residue) for cooking and heating is associated with large emissions of air pollutants in China, due to its relatively low combustion efficiency and the lack of controls. In China, the residential sector is a major contributor to emissions of anthropogenic pollutants including $PM_{2.5}$, BC, OC and NMVOCs (this sector accounts for 36–82% of the total emissions of these pollutants, according to MEIC), despite its small proportion of total energy consumption (<10%). The residential sector has been identified as a major source of uncertainty in current inventories of anthropogenic emissions in China because of the lack of reliable data and locally measured EFs [1,2,36,103].

Residential emissions in China have been estimated in many global, regional and national bottom-up emission inventories compiled using activity rates and EFs (e.g. EDGAR, [1,2,12]). These inventories typically employ activity rates (i.e. energy consumption) obtained from official sources of energy statistics, such as the China Energy Statistical Yearbook (CESY) or the International Energy Agency (IEA). Early inventories [1,2] estimated residential emissions by applying uniform EFs for a given fuel to entire sectors, due to the lack of more detailed information. However, these inventories ignore the large variations in EFs that may occur among different fuel sub-types (e.g. bituminous coal vs. anthracite coal), fuel combustion types (e.g. raw coal vs. briquette) and combustion devices (e.g. boilers, traditional stoves vs. improved stoves). In recent inventories, technology-based approaches have been adopted to better represent the dynamic changes in residential emissions in China (e.g. MEIC [34]). Lei *et al.* [34] considered dynamic changes in the share of briquettes in residential coal consumption and estimated that, because of the increased share of briquettes, the average net EFs for BC and OC in residential coal stoves decreased by 34% and 10%, respectively, from 1990 to 2005. In the MEIC inventory, the technology distribution of different coal combustion devices (i.e. boilers and stoves) in the urban residential sector was estimated using a bottom-up demand-side energy model.

Although several residential inventories have been developed for China, quantifying emissions from the residential sector remains a challenge because of the wide variety of fuel-use patterns and emission characteristics and the lack of relevant data. The estimated emissions from residential sector are much more uncertain than those from other anthropogenic sectors. Energy consumption in the residential sector is highly uncertain compared to that in other sectors. Lu *et al.* [36] assigned uncertainties (95% confidence intervals, CIs) of 33% and 80% to residential coal and biofuel use in China, respectively. Inconsistencies between provincial and national energy statistics have been reported by previous studies [25,26]. Zhang *et al.* [2] argued that coal briquettes are widely used in the residential sector; however, only a small proportion (<10%) are reported in the official energy statistics.

Alternative approaches have been developed to better understand and represent real-world fuel consumption in the residential sector. A series of surveys to assess residential energy consumption in China was carried out at the national [104,105] and regional scales [106–111]. Those survey data have provided useful information on residential fuel consumption and choices and have helped to identify their relationships with natural and socio-economic factors (e.g. temperature, household income, energy prices, fuel access, electrification and level of education). Several of these surveys [104,107,108,110,111] revealed large amounts of residential coal consumption that are missing from the current statistical system, and the emission inventories for some regions were subsequently revised based on the survey data [111]. Zhu *et al.* [112] developed regression models using climate and socio-economic parameters, including heating days and heating degree days (HDDs), to project the spatial and temporal trends in residential fuel consumption and air pollutant emissions over China.

Many laboratory and field measurements in China have been performed to assess local residential EFs. These EFs have been found to vary greatly depending on the type of fuel and the stove used, fuel quality and combustion conditions [113–123]. Based on measurements of 28 fuel/stove combinations in China, Zhang *et al.* [113] generated a database of EFs from household stoves containing species such as CO_2, CO, CH_4, TNMHCs (Total Non-Methane Hydrocarbons), SO_2, NO_x and TSPs (Total Suspended Particles) and found that the EFs associated with solid fuels were substantially greater than those of liquid and gaseous fuels. Tsai *et al.* [114] further measured the EFs of speciated NMHCs (Non-methane Hydrocarbons) for 16 fuel/stove combinations. Chen *et al.* [115] reported the EFs of particles and their carbonaceous fractions (i.e. BC and OC) for five coal briquettes burned on a residential coal stove based on measurements; they also reported the EFs for residential burning of coal chunks [116]. Li *et al.* [118] conducted field measurements to assess the emissions of carbonaceous aerosols from household biofuel combustion. Shen *et al.* [119–123] measured EFs of PM,

Downloaded from https://academic.oup.com/nsr/article-abstract/4/6/834/4775139
by guest
on 14 February 2018

Table 7. Emission factors for residential fuel combustion in China (unit: g/kg).

	Raw coal		Coal briquette			
Species	Bituminous	Anthracite	Bituminous	Anthracite	Wood	Crop residues
SO_2	0.15–20.4[a]		0.08–9.9[a,c]		0.002–0.03[a]	0.015–0.21[a]
NO_x	0.15–3.9[a]		0.07–1.1[a,c]		0.5–2[a,j]	0.23–1.7[a,j]
CO	70.7–288[a,k]		19.1–68.4[a,k]		19.7–102.7[a,i,j,m]	29.3–215.4[a,i,j,k,m]
NMVOC	0.17–6.5[a,b]		0.0003–1[a,b]		0.08–5[a,b,j]	0.18–26.6[a,b,j]
$PM_{2.5}$	0.13–46.6[a,e,f,g,k]	0.62–1.54[e,f,g]	0.03–12.9[a,c,d,f,g]	0.17–2.2[d,g,k]	0.7–8.3[a,i,l,n,o]	1.7–18[a,i,k]
BC	0.006–28.5[e,f,g,k]	0.002–0.035[e,f,g]	0.006–0.5[d,f,g,h,k]	0.001–0.012[d,g,h,k]	0.06–2.5[i,l,n,o]	0.1–2.6[i,k]
OC	0.1–17.0[e,f,g,k]	0.03–0.47[e,f,g]	0.007–10.1[d,f,g,h,k]	0.017–0.36[d,g,h,k]	0.11–4.3[i,l,n,o]	0.35–3.6[i,k]

*Data sources: [a]Zhang *et al.* [113]. [b]Tsai *et al.* [114]. [c]Ge *et al.* [124]. [d]Chen *et al.* [115]. [e]Chen *et al.* [116]. [f]Zhang *et al.* [93]. [g]Zhi *et al.* [117]. [h]Chen *et al.* [125]. [i]Li *et al.* [118]. [j]Wang *et al.* [126]. [k]Shen *et al.* [119]. [l]Shen *et al.* [120]. [m]Wei *et al.* [127]. [n]Shen *et al.* [121]. [o]Shen *et al.* [122].

Table 8. Estimates of China's residential emissions (unit: Gg/year).

Inventories	Year	SO_2	NO_x	CO	NMVOC	$PM_{2.5}$	BC	OC
Streets *et al.* [1]	2000	2523	702	43 867	5604		782	2561
Ohara *et al.* [12]	2000	2801	974	58 308			938	2497
Zhang *et al.* [2]	2001	2599	997	48 254	5996	3853	868	2254
	2006	2838	1166	55 883	7601	4461	1002	2606
Lu *et al.* [36]	2000	1947					639	1893
	2004	2048					826	2519
	2008	2365					888	2670
	2010	2931					936	2790
Zhao *et al.* [6]	2010	2888	2604	63 765		4429	809	2228
MEIC	2000	2329	741	59 820	4733	3750	721	2198
	2005	2926	988	74 799	6071	4725	869	2775
	2010	3470	1044	70 970	5704	4326	848	2481

OC and EC from the residential combustion of solid fuels under field and laboratory conditions. Most of the EFs measured in the field were higher than the corresponding EFs measured under laboratory conditions. Table 7 summarizes the measured EFs for residential fuel combustion in China, based on a literature review. As shown in Table 7, the EFs for coal briquettes are generally lower than those for raw coal. The BC EFs of bituminous raw coal are 50–200 times higher than the other EFs.

A comparison of estimates of residential emissions in China between 2000 and 2010 is shown in Table 8. Large discrepancies are associated with the SO_2 emissions in 2000 and the NO_x emissions in 2010. Ohara *et al.* [12] estimated that the year-2000 residential SO_2 emissions in China were 2.8 Tg; this value is 44% higher than that obtained by Lu *et al.* [36]. As estimated by Zhao *et al.* [6], the year-2010 residential NO_x emissions in China were 2.6 Tg; this value is 149% higher than that published by MEIC. Although large discrepancies are not observed in the emissions of BC and OC in individual years, different trends are reported by Lu *et al.* [36] and MEIC. According to Lu *et al.* [36], these quantities increased by ∼47% from 2000 to 2010; however, the corresponding estimates published by MEIC reflect increases of only 13–18%. Note that an uncertainty analysis suggests that the largest uncertainties in the residential sector are associated with the emissions of BC and OC [103].

Transportation

On-road vehicles

The air pollutants from on-road vehicles are divided into two subsectors: tailpipe exhaust and evaporative emissions. These types of emissions are discussed separately below.

Tailpipe exhaust emissions. China accounts for 14% of the world's automobiles. Reducing vehicle emissions during rapid urbanization is a major challenge in China [128]. The on-road transportation sector is the largest contributor to $PM_{2.5}$ pollution in major Chinese cities, including Shanghai, Beijing, Guangzhou and Nanjing [129–132], and this pollution has detrimental impacts on human health [133–135].

Downloaded from https://academic.oup.com/nsr/article-abstract/4/6/834/4775139
by guest
on 14 February 2018

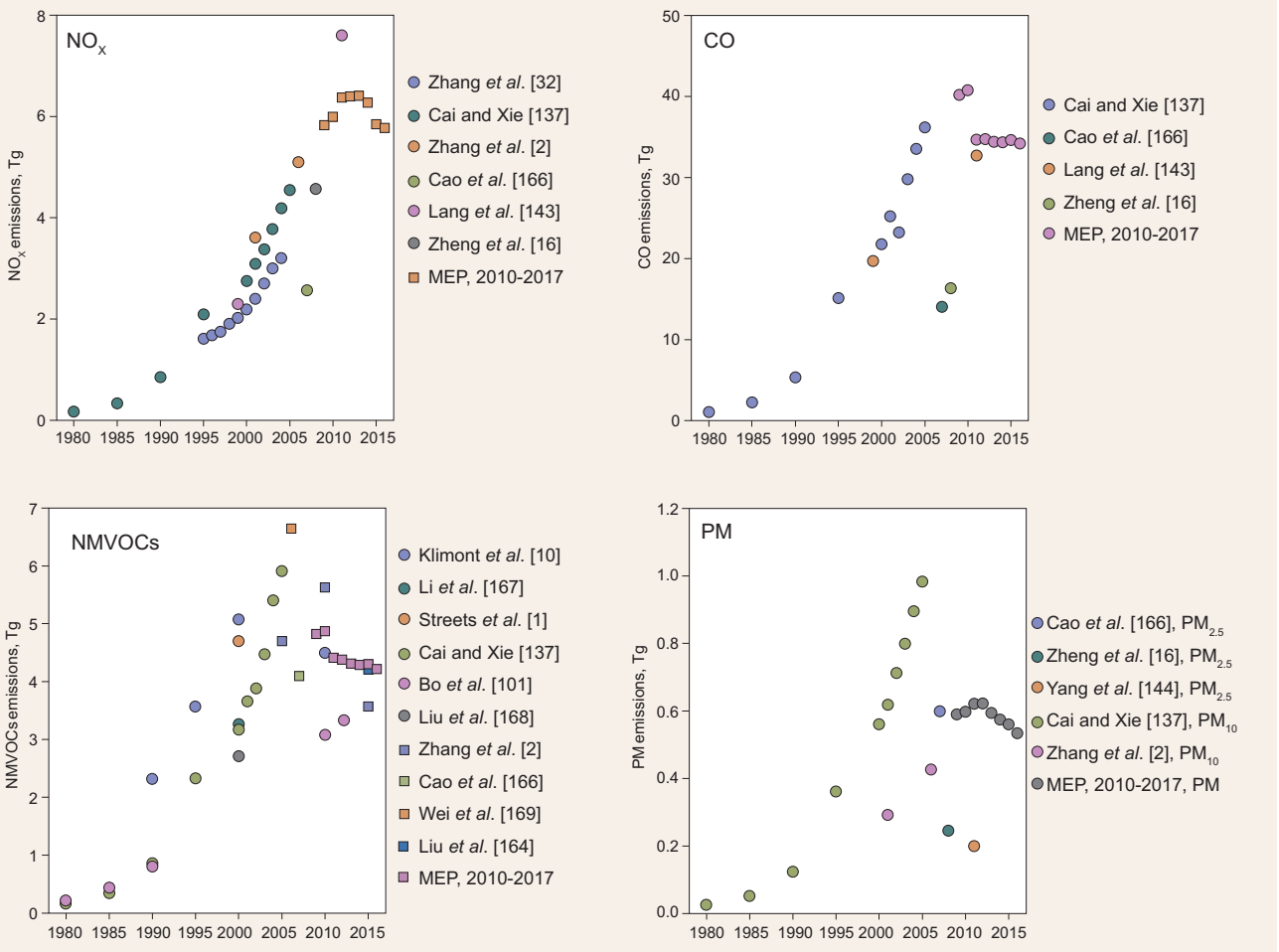

Figure 3. Summary of vehicular emission estimates in China.

Early studies of the emission estimation from on-road vehicles in China were based on data from Western countries [9,136]. During the last two decades, dozens of papers have been published that present vehicle emission inventories based on local statistics and native investigations [16,137–147]. Figure 3 presents a detailed summary of estimates of vehicular emissions. Although significant differences are seen among the different inventories, clear trends in emission reductions that were driven by progressive vehicle environmental standards are observed. The total emissions of NMHCs from vehicles peaked in approximately 2007, the emissions of CO and PM peaked in around 2010 and the total emissions of NO_x from vehicles peaked in approximately 2013 and have decreased since that time.

Local databases of EFs have been developed to reflect the real-world emission characteristics of vehicles in China. The EFs used in early studies were derived directly from international models, due to the lack of sufficient local emission testing data and comprehensive localized models. The international models from which these EFs were taken include the Mobile Source Emissions Factor (MOBILE) and Motor Vehicle Emission Simulator (MOVES) models developed by the US EPA, the International Vehicle Emissions (IVE) model developed at the University of California at Riverside and the COmputer Programme to calculate Emissions from Road Transport (COPERT). EFs from international models developed based on testing results in US or European countries do not accurately reflect the emission characteristics of vehicles in China, due to differences in vehicle configurations, ambient conditions and driving cycles. Emphasis has been placed on the localization of international models. Hao *et al.* [148] tested 171 vehicles on chassis dynamometers, and the results were used to localize the MOBILE model. Fu *et al.* [149] and Liu *et al.* [150] measured the emission rates of 12 and 75 vehicles, respectively, using portable emission measurement systems (PEMS); the testing results were used to localize the MOBILE and IVE models, respectively. Zhang *et al.* [151]

Downloaded from https://academic.oup.com/nsr/article-abstract/4/6/834/4775139
by guest
on 14 February 2018

developed an updated EF model for the Beijing vehicle fleet (EMBEV) that was based on large amounts of testing data produced by a comprehensive vehicle emission testing programme. The failure to represent real-life driving cycles in the laboratory, which significantly lowered the accuracy of emission estimates, revealed the presence of 'lab-to-road' issues that arise from erroneous driving cycles or the disabling of pollution control devices [152]. The importance of real-world emission testing has increased in recent years. Investigations based on the PEMS testing programmes led by the Tsinghua University, Beijing Institute of Technology (BIT) and Vehicle Emission Control Centre (VECC) teams, as well as other researchers, have been launched, and the results of these investigations represent a comprehensive database of real-world EFs [150,151,153–161].

The accuracy of activity rates is another key factor that affects the quality of vehicular emission inventories. Activity levels are primarily calculated using the number of vehicles registered and vehicle kilometres travelled (VKT) data. The vehicle registration data can be obtained from public statistics and contain relatively low uncertainties. To provide reliable activity level data, representative and accurate VKT data are of great importance. Approximately 80–2000 samples have been investigated in China [144,162,163]. Liu *et al.* [164] derived vehicle activity data from the trajectories of more than 70 000 cars and the annual mileages of 2 million trucks in China; this study represents an important step towards improved emission estimates.

In addition to the emission estimates, the gridding of emissions significantly affects the accuracy of emission inventories for the transportation sector. Most existing studies employ parameters such as GDP (Gross Domestic Product), road length, population, city lights and vehicle stocks as spatial proxies to allocate emissions to individual grid cells [38,137]. Zheng *et al.* [16] developed emissions using county-level geographical parameters; these county-level emission estimates were then allocated to grid cells using the China Digital Road Network Map (CDRM). Integrating traffic flow data into the development of high-resolution vehicle emission inventories has been investigated by several studies [139,147,163,165]. In addition, vehicle registration data can be employed in estimating emissions from passenger cars; however, these data cannot be used for freight trucks that often travel long distances between cities and provinces. Yang *et al.* [144] developed a road emission intensity-based (REIB) approach to better describe the spatial distribution of truck emissions in China.

The development of future vehicle emission inventories requires additional real-world emission testing data collected under different ambient conditions (e.g. high altitude) and driving conditions (e.g. cold start). The MEP should utilize the second national pollution census to launch more testing programmes to enhance the EF database. Detailed traffic flow data are needed to improve the accuracy of vehicle activity rates and the spatial distribution of emissions.

Evaporative emissions. Emissions of NMVOCs from vehicles, including tailpipe exhaust and evaporative emissions, have become a major and growing source of NMVOC emissions in China [21,131,170–172]. Vehicular evaporation has joined tailpipe exhaust as a dominant pathway of vehicular NMVOC emissions, due to the limited controls on evaporation losses [173,174]. Previous studies used the ratios of toluene and benzene concentrations (T/B) to evaluate the contributions from vehicle sources to ambient NMVOCs. The T/B ratios of tailpipe exhaust are typically 2.0; higher ratios are observed in evaporative emissions in Asia, due to the elevated toluene concentrations in gasoline. The T/B ratios in most urbanized areas are high, e.g. 37 in Hong Kong, 10 in Manila and Bangkok and 6 in Seoul, indicating contributions from evaporative emissions [175–178].

Evaporative sources include the venting of canisters and fuel permeation/leakage. Based on certified test procedures, evaporative emissions can be divided into those from refuelling, hot soak, diurnal and running loss, listed in order of decreasing amounts emitted. Speciation profiles have been constructed using headspace vapour [179,180], liquid fuel [180,181], tunnel tests [182] and Sealed Housing for Evaporative Determination (SHED) tests [183]. Liu *et al.* [164] detected 93 species of NMVOCs and determined their individual shares in emissions produced by different processes, mechanisms and vehicle control technologies. Furthermore, a comprehensive vehicle activity-based speciation profile was developed that includes the 35 major NMVOC species that account for 90.6∼98.6% of total detected organics. Studies of such EFs are highly complex, considering the evaporative nature of fugitive emissions; the methods used to determine these EFs include SHED tests and tunnel tests. The former type of test is more accurate and widely used. Pang *et al.* [184] reported evaporative EFs for 49 in-use vehicles from fleets ranging from 1999 to 2003 in the USA. Mellios *et al.* [185] tested four vehicles in Europe to validate existing evaporative emission results. Liu *et al.* [174] evaluated emission rates in China using 30 crossover tests performed on five tested vehicles using non-ethanol gasoline and 41 crossover tests performed on five vehicles

Downloaded from https://academic.oup.com/nsr/article-abstract/4/6/834/4775139
by guest
on 14 February 2018

using four concentrations of ethanol-blended gasoline (0–10%). Four types of local EFs—diurnal, hot soak, permeation and refuelling—were provided. The evaporative emission rates from Euro4 vehicles (which have diurnal evaporative emission rates of 2–8 g/day) are dozens of times those of vehicles in the USA (0.3 g/day), reflecting a substantial gap between these two sets of regulations. An ethanol concentration of 10% can lead to increases in evaporative emissions of 20–40%.

Models of evaporative emissions are either based on the Wade-Reddy equation, which considers changes in various factors (including gasoline volatility, ethanol content, canister size, canister load, canister purging, vehicle, fuel system design, fuel tank fill level, parking and driving patterns, absolute ambient temperature, temperature variations and ambient pressure), or are determined directly from experimental results. The former approach has been used in several well-known models, such as MOVES, MOBILE and IVE [186]. Studies that employ these models include Huang *et al.* [187] (IVE model), Dong *et al.* [188] (Wade-Reddy equation with consideration of the impact of parking activities) and Yang *et al.* [189] (Wade-Reddy equation). The latter approach has been used in the studies by Mellios and Samars (simulation of final diurnal emissions) [185,190], Yamada (24-hour diurnal and hot soak emissions) [173] and Liu (72 hour diurnal and hot soak, refuelling and permeation emissions) [164,174]. In 2015, the evaporative emissions of volatile organic compounds (VOCs) in China ranged from 185 Gg in 2010 to 264 Gg. These emissions correspond to approximately 0.12–0.21 g/km, excluding running losses and motorcycles [164,189], and are greater than the Euro3 tailpipe emission rate (0.19 g/km) [174]. Liu *et al.* [164] estimated total running losses of 1146 ± 768 Gg in China. Evaporative emissions from vehicles (including motorcycles) are responsible for 39.2% of the total vehicular emissions of NMVOCs [164]. The largest uncertainty is due to the lack of direct evidence for the magnitude of running losses in China. Other major uncertainties in current evaporative inventories of China are due to the lack of consideration of driving and canister conditions before parking, which lead to differences between actual EFs and those measured in the laboratory.

Off-road engines

Off-road equipment is usually diesel-fuelled in China. Unlike on-road vehicles, little attention has been devoted to this subsector. Recent studies indicate that the emissions of NO_x and PM from off-road engines are comparable or even higher than those of on-road vehicles [191,192]. Wang *et al.* [192] provided an overview of the methodology, EFs and emission estimates for five major contributing sources: agricultural equipment, industrial equipment, shipping, locomotives and commercial airplanes. Shipping emissions are illustrated separately in the following subsection, followed by a summary of other off-road sources.

Shipping. Increased connectivity and the international marine trade have stimulated inland development. In 2015, 41% of the cargo loading and 60% of the unloading of the world marine trade occurred in Asia [193]. China is one of the largest shipping countries and has more than 18 000 km of coastline and over 50 ports. These ports are primarily located within five port clusters, namely the Pearl River Delta (PRD), the Yangtze River Delta (YRD), the Bohai Rim Area (BRA), the south-east coast and the south-west coast. Seven of the top 10 container ports in the world are located in China. Specifically, these ports are those of Shanghai, Shenzhen, Ningbo, Hong Kong, Qingdao, Guangzhou and Tianjin (http://www.worldshipping.org/).

The establishment of port-level and regional shipping emission inventories is an urgent priority. The fuel-based method [194–198] applies to calculations that apply to large scales and overlong time scales, whereas the trade-based method [199] requires less data but produces results with greater uncertainty. Both of those methods are categorized as top-down approaches, and their results are generally of lower accuracy compared to those of bottom-up ones, which derive their estimates from the characteristics and movements of ships [200]. The vessel-visa-based method is a bottom-up approach that is based on ship visa registration data; it was used predominantly in earlier studies of port-scale or port-cluster-scale emissions [194–197]. The automatic identification system (AIS)-based method is the most advanced; it is based on the movements of individual vessels. The AIS-based method has been used in recent studies to obtain emission inventories with high spatial resolutions.

The national-level ship emission inventory has been continuously developed in the past two years. Liu *et al.* [201] obtained the first estimates of emissions from ocean-going vessels (OGVs) in East Asia using an advanced method based on detailed dynamic AIS data; the climate impacts of the associated radiative forcing and the health impacts and premature deaths caused by ship emissions were also assessed. Chen *et al.* [202] developed a comprehensive national-scale ship emission inventory in China for 2014 based on AIS data, including OGVs,

Downloaded from https://academic.oup.com/nsr/article-abstract/4/6/834/4775139
by guest
on 14 February 2018

Table 9. Shipping emissions in China (unit: Gg/year).

		Air pollutants										
Region	Port	SOx	PM_{10}	$PM_{2.5}$	NO_x	CO_2	CO	VOC	HC	Base year	Method	Reference
East Asia/	/	1850	240		2800	126 000	108		100	2013	AIS	Liu *et al.* [201]
China	/	1194	181	167	2208	78 430	242		112	2014	AIS	Chen *et al.* [202]
China	/	1300			1910	86 300	74		69	2013	AIS	Fu *et al.* [203]
YRD	Regional	380			710					2010	AIS	Fan *et al.* [204]
	Shanghai	82	12.3	11.4	152		7.1			2010	AIS	Fan *et al.* [204]
	Shanghai	35.4	4.6	3.7	57	289	4.9		2.1	2010	Fuel-based, vessel-visa data	Fu *et al.* [197]
	Shanghai	51		7	58	3013			4.6	2003	Fuel-based, vessel-visa based	Yang *et al.* [194]
	Ningbo-Zhoushan	21.6	2.6	2.4	35		3	1.5		2010	AIS	Yin *et al.* [219]
	Yangshan	5.6	0.22	0.86	10.8	578	1.1			2009	AIS	Song *et al.* [220]
	Estuary of the Yangtze River	147			245	4054	57		9	2010	AIS	Yao *et al.* [221]
GPRD	Regional	104			150					2015	AIS	Mao *et al.* [206]
PRD	Regional	62	7.2	6.6	104		10.6	4.2		2013	AIS	Li *et al.* [205]
	Regional	63	2.3		92		10.5	0.9		2006	Fuel-based	Zhang *et al.* [196]
	Shenzhen	1.6	0.16	0.15	6.7	1.6	0.7		0.08	2003	Trade-based	Li *et al.* [199]
	Shenzhen	13.6	2.2	1.7	23.3		2.2	1.1		2010	AIS	Yang *et al.* [222]
	Hong Kong	12.4	1.4		14.5		1.4	0.6		2007	AIS	Ng *et al.* [223]
	Hong Kong	8.2	1		17.1					2007	AIS	Yau *et al.* [224]
	Guangdong Province	146	7.9	7.2	231		30	9.3		2010	Fuel-based. vessel-visa based	Ye *et al.* [198]
BRA	Regional	121			174	7209	14.4		6.1	2014	AIS	Xing *et al.* [225]
	Regional	231	21.5	19.7	306	13 344	23.8		9.9	2013	AIS	Song *et al.* [226]
	Tianjin	29.3	4	3.7	41.3		3.6	1.7		2014	AIS	Chen *et al.* [227]
	Tianjin		0.2		4.3		0.7		0.2	2006	Fuel-based	Jin *et al.* [195]
	Tianjin	61	5.4	4.9	73	3471	5.7		2.4	2013	AIS	Xing *et al.* [225]
	Qingdao	33.2	4.5	4.2	42.9		3.7		1.9	2014	AIS	Chen *et al.* [228]
	Qingdao									2004	Vessel-visa based	Liu *et al.* [229]
	Tangshan	80	7.6	7	112	4620	8.7		3.6	2013	AIS	Xing *et al.* [225]
	Qinhuangdao	64	6	5.5	86	3727	6.7		2.8	2013	AIS	Xing *et al.* [225]
	Huanghua	26.3	2.5	2.3	34.6	1526	2.7		1.1	2013	AIS	Xing *et al.* [225]
	Dalian	49.4	5.8		52	2885	4.7		2	2012	AIS	Tan *et al.* [230]
Taiwan	Kaohsiung	0.64	0.053	0.049	0.68	34.8	0.053		0.019	2012	AIS	Cullinane *et al.* [231]
	Keelung	0.19	0.016	0.014	0.2	10.19	0.016		0.006	2012	AIS	Cullinane *et al.* [231]
	Taichung	0.27	0.022	0.02	0.28	14.4	0.022		0.008	2012	AIS	Cullinane *et al.* [231]

coastal vessels (CVs) and river vessels (RVs); moreover, the emission characteristics were discussed from various perspectives, such as vessel type, operating mode, discharge equipment, monthly variations and the spatial distributions. Fu *et al.* [203] compiled national- to port-level emission inventories for China, hotspot regions and individual ports and compared ship emissions with on-road mobile source emissions.

Estimates of the shipping emissions from the abovementioned sources for various regions are presented in Table 9. The total shipping emissions of SO_2, NO_x and PM determined using bottom-up inventory methods are 1300, 1910 and 164 Gg/yr in the year 2013 [203] and 1193.7, 2208.4 and 347.2 Gg/yr in the year 2014 [202]. The largest body of contributions regarding shipping emissions addresses ships in the YRD [204]. This region includes emissions from the ports of Ningbo-Zhoushan and Shanghai, as well as 13 other ports. The largest sources are container ships. Of the other types of ships, the dominant emitters depend on the location. Non-container cargo ships contribute 32–36% of emissions in the YRD [204], whereas bulk carriers contribute approximately 17.5% of emissions in the Jing-Jin-Ji (JJJ) region [202] and 14–20% of emissions in the PRD [205,206]. Variations in emission amounts are difficult to explain, given the variability in domain size, the raw data and methods used, and the target year.

The biggest challenge in the future development of emission inventories is the unreliability of EF data. Current emission inventories in China usually adopt ship EFs from mainstream reports,

Downloaded from https://academic.oup.com/nsr/article-abstract/4/6/834/4775139
by guest
on 14 February 2018

including those of the International Maritime Organization [207,208], Entec [209], Energy and Environmental Analysis Inc. [210], the EPA [211], ICF International [212] and EDGAR. Despite the consistency of the SO_2 (9.6–10.6 g/kWh), PM and NO_x EFs are of large uncertainties (1.2–1.5 g/kWh for PM and the emission regulation threshold is used for NO_x). Measurements of in-use ships in China improved the local EF database in several studies [213–216]. The measured EFs in China are insufficient to build an emission inventory because (i) the sample size is suboptimal (seven ships were tested in Fu *et al.* [213] and Peng *et al.* [215], three ships were tested in Zhang *et al.* [216] and one ship was tested in Lou *et al.* [214]) and (ii) the engine sizes on the measured vessels are much smaller than the fleet average of OGVs; the researchers tested ships with main engines ranging from 76 to 2648 kW [213–216]—much lower than the fleet average of cargo vessels for 2001 (4975 kW) determined from the Lloyd's Maritime Information System [217]. Difficulties encountered in the systematic establishment of EFs include on-board monitoring of international ships and measurement authorization. Inconsistent results were seen in determining the total emissions of PM (0.72∼9.4 g/kg with fuel sulphur content of 0.05% [216], 1.5–3.2 g/kg with 0.2% sulphur [215]), NO_x (35.7∼115 g/kg [216], 64.1∼83.9 g/kg [215]) and CO (6.93∼30.3 g/kg [216], 30.7∼51.7 g/kg [215]); the total emissions of HC were 1.4–4.4 g/kg with a fuel sulphur content of 0.2% [215].

AIS data display large uncertainties, especially in Asia. AIS data include satellite-based and territory-based signals. Low earth orbiting satellites record information on ships on the high seas; however, the coverage is lower in Asia than in North America or Europe [208]. The signal intervals are also longer in Asia than elsewhere, occasionally exceeding multiple days. Territory-based stations are distributed near shore and generally display satisfactory signals for offshore areas; however, difficulties in data access and coverage evaluations occur in Asia. Fortunately, AIS data coverage in Europe has been observed to be increasing [218], emphasizing the importance of updating shipping emission inventories using the latest AIS data.

The statistical database of ships is also a limiting factor. In the series of studies by Liu, the number of documented ships with detailed statistical information increased from 65 903 to 71 058; however, missing information still caused considerable uncertainties: (i) 8% of the ship records could not be matched, given the absence of a Ship Identification Number; (ii) inconsistent properties were noted for 30% of the ships, such as the vessel type, rated engine speed, rated engine power, length, width, height, design maximum speed, dead weight tonnage (dwt), maximum draught and build year; a gradient-boosting regression tree approach (GBRT) was adopted in the studies by Liu [201] to solve this problem; (iii) many smaller vessels and fishing vessels were not entered in either Lloyd's Register or the China Classification Society database. Thus, although uncertainties are known to exist at the fleet aggregate level, the magnitudes of these uncertainties are unknown.

A cross-study comparison of shipping emissions with port function, the urban population and economic development would be invaluable and would reveal the impacts of various factors and their relationships with the differentiation of regional shipping emissions. In addition, shipping emission inventories should be used broadly in impact evaluations of air quality, health and climate. A thorough evaluation is necessary to guide the development of future policies and regulations.

Other off-road sources. The emissions from agricultural equipment, construction machinery, locomotives and off-road vehicles are mainly estimated based on fuel consumption and the corresponding EFs. The populations of agricultural equipment and construction machinery, the quantities of freight transported by locomotives and the sales of three-wheelers and low-speed trucks can be obtained from the Chinese statistical yearbooks. Several studies report the activity rates for various sources: Fan *et al.* [232] for different types of agricultural equipment, Fu *et al.* [233] and Ge *et al.* [234] for harvesters and agricultural tractors and Li *et al.* [235] for typical construction equipment. Fuel consumption is then calculated based on the average fuel consumption rate for each activity. Wang *et al.* [192] estimated that, in 2012, agricultural equipment, industrial equipment and locomotives consumed 37.1, 5.2 and 3.7 Tg of diesel fuel, respectively.

These EFs may vary with working conditions, the engine technologies deployed and the emission standards that are in force; thus, in-field measurements of EFs are needed in China. However, most of the EFs used are extracted from existing EF models, such as NONROAD, which was developed by the US EPA. Local studies that characterize the emissions from off-road engines are rare. Representative EFs that are currently used for inventory development can be found in Wang *et al.* [192].

Off-road emissions in China are far from accurately quantified and validated. Agricultural machinery (harvesters, agricultural tractors, etc.) makes the largest contributions to NO_x emissions, followed by vessels (see the above subsection) and

Downloaded from https://academic.oup.com/nsr/article-abstract/4/6/834/4775139
by guest
on 14 February 2018

industrial equipment; specifically, agricultural machinery emits 1744 Gg of NO_x and 147 Gg of PM annually [192]. Very large gaps exist in estimates of emissions from off-road sources in China. Real-world characterizations of both activity rates and EFs are urgently needed.

Solvent use

Solvent use contributes more than 20% of the total emissions of NMVOCs in China [10,28,100]. Emissions due to solvent use are estimated based on the 'EF' method, which relies on the activity rates and EFs for each source category. The major sources include the industrial use of paint for vehicles and architectural walls, industrial adhesives, printing, degreasing, pesticide use, pharmaceutical production and dry cleaning. Activity data for solvent use mainly indicate paint consumption, production output, vehicle number and population, which can be obtained from the statistical yearbooks or the reports of the NBS and domestic industrial associations [2,10,100–102,169,236–237].

Current studies that employ EFs refer mainly to Klimont *et al.* [10], Wei *et al.* [100] or Bo *et al.* [101]. Klimont *et al.* [10] developed the first long-term inventory of NMVOC emissions over China using properly revised European EFs, due to the lack of local information. Wei *et al.* [100] provided summary values of local EFs associated with paint use in vehicle manufacturing, printing and decorative paint use. For sources in which the solvent content is limited by nationwide regulations or standards in China, the limiting value is used (see below). Other EFs are based on data from Western countries obtained from the European Monitoring and Evaluation Program/European Environment Agency (EMEP/EEA) guidebook. Bo *et al.* [101] estimated emissions using EFs derived from the US AP-42 database. Wu *et al.* [102] updated the EF database with locally measured EFs for solvent use in pharmaceutical production, vehicle paint use, the manufacturing of cans and enamelled wire, and household appliances. These EFs, which include up-to-date local EF data in China, are summarized in Wu *et al.* [102].

To suppress the dramatic growth in emissions of NMVOCs, the government of China has imposed limits on solvent contents, thus providing a reference in the determination of EFs. Up to 2015, the nationally regulated sources included wood paint by GB 18581–2009, interior wall paint by GB 18582–2008, water-based solvents for architecture and industrial paints by HJ 2537–2014, indoor adhesives by GB 18583–2008, vehicle paint by GB 24409–2009, wood production by HJ 571–2010, leather products by HJ 507–2009, textile products by HJ 2546–2016, solvent-based wood furniture finishes by HJ/T 414–2007, printing ink by HJ 2542–2016, HJ/T 371–2007 and HJ 567–2010, and household detergents by HJ 458–2009. More local surveys and independent validations are needed to determine the effects of applying this legislation nationwide and to better quantify the emissions of NMVOCs associated with solvent use.

Agriculture

China may be the largest emitter of atmospheric ammonia in the world. However, the annual emissions reported by researchers vary from 9.8 to 17.2 Tg [1,13,238,239], implying that these estimates contain large uncertainties. Because of the very large demand for agricultural products, the application of synthetic nitrogen fertilizer and the management of livestock manure dominate ammonia emissions in China [240]. Accurate estimation of the emissions nationwide is difficult because farming practices (e.g. fertilizer application methods, animal housing conditions and animal manure management) and environmental conditions that determine ammonia volatilization (e.g. surface temperature, soil acidity, soil water content and wind speed) are regionally diverse.

A mathematical model that is applicable to all of China, together with local EFs, is needed for realistic estimates. Huang *et al.* [238] attempted to develop a simple multi-parameter model and Huo *et al.* [241] derived ammonia EFs for urea, ammonium sulphate and compound fertilizer based on a field experiment performed on croplands planted with winter wheat in northern China. Moreover, satellite retrievals [242,243] and model inversions [244] have also been used to constrain ammonia emissions. Note that the Infrared Atmospheric Sounding Interferometer aboard the European MetOp satellite and the Atmospheric Infrared Sounder aboard NASA's Aqua satellite are capable of providing more detailed spatial patterns and temporal trends than ground measurements. To better estimate the ammonia emissions in China, more in-field measurements should be conducted to reflect real-world conditions of fertilization and animal manure management in China.

In-field crop residue burning

In-field crop residue burning (also referred as agricultural fire) is the predominant type of open biomass burning that is conducted in China, and it occurs mainly during the harvest season. Emission

Downloaded from https://academic.oup.com/nsr/article-abstract/4/6/834/4775139
by guest
on 14 February 2018

estimates for this subsector obtained using various methods have frequently been reported. These emissions can be calculated as the product of crop yields, the residue-to-production ratio, the dry matter-to-crop residue ratio, the percentage of dry matter burned in the fields and EFs [245]. This method requires multiple parameters, and the results incorporate significant uncertainties. Although MODIS (Moderate Resolution Imaging Spectroradiometer) sensors aboard polar-orbiting satellites can capture the spatial patterns of agricultural fires well, it has been found that many fire events are likely not identified in China because the resolution of these data is still too coarse to pinpoint the small fires that commonly occur on croplands in China [246]. Randerson *et al.* [247] proposed a method to estimate the areas burned by small fires using the active fire data. Wooster *et al.* [248,249] found a strong linear relationship between time-integrated fire radiative power (FRP) and the amount of biomass combusted; thus, in recent years, FRP has been suggested as a new tool for estimating the emissions from vegetation fires [250,251]. This method is almost independent of the characteristics of local biomes and may produce realistic estimates. Liu *et al.* [252] used an FRP-based method to estimate the emissions from crop residue burning in northern China. In addition, geostationary satellites (e.g. Himawari-8) can assist in better characterizing the FRP diurnal cycles of agricultural fire events in China [253].

EVOLUTION OF EMISSIONS IN CHINA

Using the updated methods and input data for each sector described in the previous sections, significant improvements in total emission estimates have been made during the last several decades. As is reasonable, emission estimates differ among inventories, due to differences in the compilation methods and data used [254]. Recognizing these differences, we focus here on reviewing the best available knowledge of the emission characteristics of pollutants, as well as their sectoral distributions and historical trends between 2000 and 2015 in China; we also examine future projections of emissions to 2030. The sectoral distributions of the emissions of each pollutant are shown in Table 1, and the changes in emissions from 2000 to 2015 derived from various studies are shown and compared in Fig. 4. The year 2010 is chosen for use as a reference year in the following analyses.

SO_2

SO_2 can cause adverse effects on air quality, human health and ecosystems. SO_2 emissions in China are estimated to have been 18–28, 29–35, 24–31 and 22–29 Tg in 2000, 2005, 2010 and 2014, respectively (derived from literature in Fig. 4). From 2000 to 2006, SO_2 emissions in China increased by 53–65% at an annual growth rate of 7.3–8.7% [13,36,255] (EDGAR v4.2 (available at http://edgar.jrc.ec.europa.eu/), MEIC v1.2 (available at www.meicmodel.org)). The growth of emissions began to slow in approximately 2005; emissions then decreased after 2006, due to the nationwide use of FGD systems in power plants [36,47]. The annual growth rate of SO_2 emissions for the period of 2006–10 was –4.6%, according to the MEIC dataset; this value reflects the efficacy of the control measures implemented during the 11th Five-Year Plan (FYP). During the 12th FYP, the 8% emission reduction target was achieved (a 14% reduction was realized, according to MEIC). The SO_2 emission trends are in good agreement with satellite and ground-based observations [36,44,256–259].

SO_2 emissions are dominated by the power and industrial sectors. In 2010, power plants and industry contributed approximately 8 Tg (27%) and 16 Tg (58%) to the total emissions, respectively. The fractional contribution of power plants decreased from 49% in 2006 to 27% in 2010. The emissions from power plants decreased by approximately 9 Tg during the same period, due to the installation of FGD systems, the construction of large units and the decommissioning of small units; these steps were taken to achieve the planned 10% reduction in emissions during the 11th FYP period [19]. On the other hand, control measures are still lacking in industrial sources. The industrial combustion sector became the largest contributor (more than 50%) to the total emissions after 2008.

The sulphur content of fuel, fuel use, the degree of sulphur retention in hard coal and the actual removal efficiency of FGD systems are the main factors that contribute to the uncertainties in SO_2 emissions [36]. Liu *et al.* [19] developed a unit-based coal-fired power plant emission inventory based on the CPED; this inventory reduced the uncertainty range in SO_2 emissions to –22 to 23%. Due to the large contributions from industrial coal combustion, SO_2 emissions are quite sensitive to uncertainties in energy statistics [26].

Energy-saving measures are increasingly important for achieving further SO_2 emission reductions by 2030. Under the current emission control strategy, SO_2 emissions will increase by 26% or 37% [7,8]. The enforcement of energy-saving measures and progressive end-of-pipe control measures are projected to lead to reductions in SO_2 emissions of 36% and 26%, respectively, compared with a baseline scenario. The reduction potential associated

Downloaded from https://academic.oup.com/nsr/article-abstract/4/6/834/4775139
by guest
on 14 February 2018

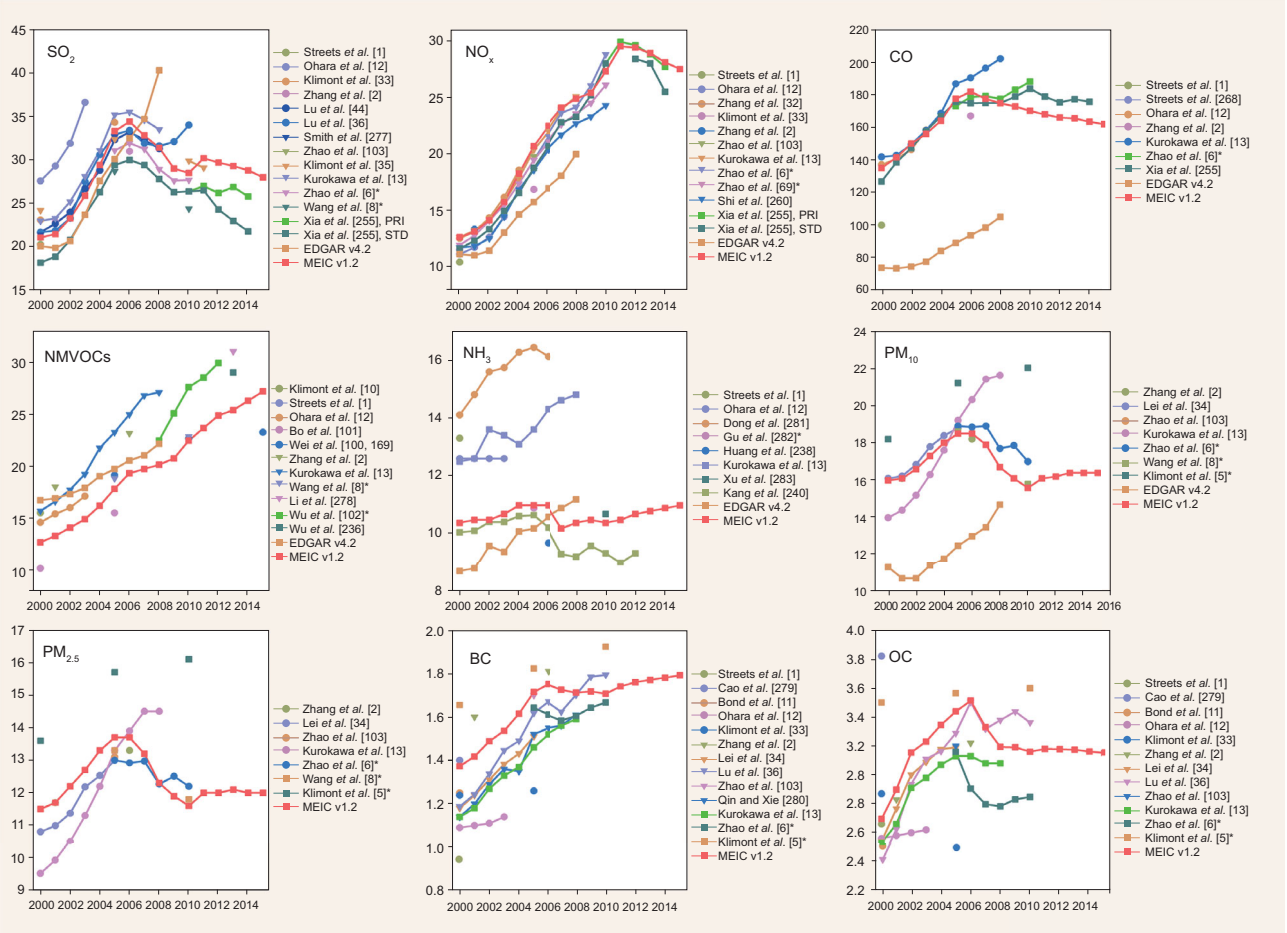

Figure 4. Evolution of emissions from 2000 to 2015 in China (Unit: Tg). References marked with ∗ are emission estimates including agricultural waste field burning. 'Xia *et al.* [255], PRI' and 'Xia *et al.* [255], STD' are two cases of emission estimates regarding to the pollutant control devices and further environmental standards, respectively (Xia *et al.* [255]).

with the installation of end-of-pipe control technologies will decrease, highlighting the importance of energy-saving measures in achieving further reductions in SO_2 emissions.

NO_x

NO_x ($NO+NO_2$) plays a key role in the formation of ozone and secondary aerosols. The emissions of NO_x in 2010 are generally consistently estimated to have been 26–29 Tg [7,8,69,255] (MEICv1.2). Power plants, industry and transportation are the major contributors to the total emissions, and these sectors have shares of 28–34%, 34% and 25%, respectively [69,260] (MEICv1.2). The power and transportation sectors contributed 9 and 7 Tg to the total emissions in 2010, respectively (MEICv1.2). The industrial sector has become the main contributor since 2010. The sector distributions remain relatively stable, although the industrial sector displays increases, whereas the power sector displays decreases [3].

Driven by the rapid economic development and the lack of relevant emission controls, NO_x emissions increased during both the 10th FYP and the 11th FYP [12,13,32,69] (EDGAR v4.2, MEICv1.2). The rate of growth in NO_x emissions was 10.3% from 2000 to 2005 and 5.7% from 2005 to 2010 (MEIC v1.2). The rapid increases in NO_x over China during this period are confirmed by satellite-based observations [258,261–266]. During the 12th FYP, the government of China set a target of reducing NO_x emissions in 2015 by 10% compared to 2010. To achieve this goal, end-of-pipe pollutant abatement strategies were carried out nationwide for the power, industry and transportation sectors, and these strategies tended to be effective in controlling NO_x emissions [7,69]. From 2011 to 2015, a decrease in emissions of 21% is estimated to have occurred, consistent with the changes in NO_2 columns measured by satellites

Downloaded from https://academic.oup.com/nsr/article-abstract/4/6/834/4775139
by guest
on 14 February 2018

[267]. The power sector was the primary contributor to these emission reductions; in this sector, a 56% reduction is estimated to have been realized in this period. This reduction is associated with the increase in the penetration of SCR systems from 18% to 86%. The release of emission standards for vehicles also had a significant effect in terms of limiting emissions, especially in the urbanized regions, such as Beijing and Shanghai [267].

It is predicted that dramatic reductions in emissions of NO_x can be achieved if end-of-pipe facilities are installed and stringent vehicle standards are applied in 2030. Zhao *et al.* [7] predict that the NO_x emissions will decrease by 20% from 2010 to 2030 in a best-guess scenario, and they will be further reduced 24% if the issued and proposed emission standards are fully achieved. Six scenarios that combine two energy scenarios and three sets of end-of-pipe pollution control measures were designed by Zhao *et al.* [69] to predict the trends in NO_x emissions from 2010 to 2030. By 2030, NO_x emissions are projected to increase by 36% in the baseline case. In the most stringent control scenario, in which SCR/SNCR systems installed and stringent vehicle standards are applied, emissions would decrease by 61% compared to the 2010 level. This reduction was updated by Wang *et al.* [8] to 72% using the same prediction framework.

CO

CO is emitted by incomplete combustion and is a precursor of ozone formation. Streets *et al.* [268] and Zhang *et al.* [2] carried out two pioneering investigations that improved the accuracy of estimates of CO emissions in China. With the exception of EDGAR, emission estimates are generally consistent among the inventories shown in Fig. 4. EDGAR estimates much lower CO emissions because it underestimates fuel consumption by the residential sector [254]. According to the MEIC dataset, emissions of CO increased from 135 to 177 Tg (+31%) for the period of 2000 to 2005 and then decreased from 182 to 170 Tg (–6%) from 2006 to 2010. The decrease in CO emissions during 11th FYP is attributable to improvements in combustion efficiency, the recycling of industrial coal gases and strengthened vehicle emission standards [3]. The annual growth rate associated with the downward trends in CO emissions was estimated to be –1.2% per year, which agrees well with multiple satellite datasets [269–271]. From 2011 to 2015, emissions of CO continue to decrease by 4% and are reduced by as much as 162 Tg in 2015 (MEIC v1.2).

The sectoral distributions of CO emissions are relatively stable from 2000 to 2015. The industrial and residential sectors are the main contributors and are estimated to have emitted 75 Tg (44%) and 71 Tg (42%) of CO in 2010, respectively (MEICv1.2). Industrial emissions of CO increased by more than 50% from 2000 to 2008, due to the production of steel, coke, cement, bricks and other materials. Since 2008, CO emissions from industrial sources have decreased, mainly due to the recycling of coal gas in plants and the substitution of shaft kilns in cement production. Residential emissions began to decrease after 2007 because of the reduced consumption of coal and biofuels in households [13]. The transportation sector contributed 12% of the total emissions in 2010. Due to the implementation of stringent vehicle emissions standards, the share of transportation has decreased since 2006.

Further reductions in CO emissions could be achieved through improving combustion technologies in the future. CO emissions from cement production, which contribute approximately 8% of the total, are estimated to decrease by between 32% and 63% in 2020 compared to 2010, due to the continuing promotion of rotary kilns and the closure of shaft kilns [15].

NMVOCs

NMVOCs are crucial precursors in the formation of tropospheric ozone and secondary organic aerosols. Given the important role of NMVOCs in air pollution control, NMVOC emissions have received increasing attention in recent years.

Due to the rapid economic development and the lack of strong control measures, the national emissions of NMVOCs in China rose continuously from 2000 to 2015. The annual growth rate associated with this rapid increase in emissions from 2000 to 2005 is estimated to have been 7.0% and 8.9% [101,13] (MEIC v1.2). From 2005 to 2010, the emissions of NMVOCs increased at a relatively slow annual rate of 3.4–4.6% [8,169] (MEIC v1.2). The results of Wu *et al.* [102] reflect emissions of 22.4 Tg in 2008 and 29.8 Tg in 2012 and an annual growth rate of 7.4%—higher than the 5.3% estimated by MEIC v1.2.

The contributions of different sources to total NMVOC emissions vary among different studies. Industrial processes and transportation are two of the primary contributors, and they account for 29.3–39.9% and 25.6–26.9%, respectively, from 2008 to 2013, as estimated by Wu *et al.* [102,236]. In contrast, MEIC v1.2 indicates that NMVOC emissions are produced primarily by industry (35% in 2010),

Downloaded from https://academic.oup.com/nsr/article-abstract/4/6/834/4775139
by guest
on 14 February 2018

residential biofuel combustion (22%) and solvent utilization (32%) [3]. In MEIC, the contributions from the residential sector and solvent use (22% and 32%, respectively) are much higher than in the results presented by Wu *et al.* [102] (10% and 15%), whereas the proportion of transportation is much lower in MEIC (10%). These discrepancies in the sector-based NMVOC emissions can be attributed to the differences in the source classification system, activity rates and EFs used in the two inventories. Combining the results of current studies, we conclude that the industrial sector (especially the petroleum-related industry and the coke industry) makes the largest contribution to the total emissions and was also the major driving source of the rapid increase in emissions since 2008. The combustion of biofuels in the residential sector, the use of solvents (especially in paint, adhesives and pesticide use) and transportation are other key contributors.

More reliable EFs are needed to reduce the uncertainties associated with NMVOC emissions. In recent years, increasing numbers of local EFs have been measured; these factors address biofuel combustion, coke production, rubber products and other emission sources. However, most of the relevant EFs still rely on foreign databases, such as AP-42 or the EEA handbook (see the 'Petroleum industry' and 'Solvent use' sections). More measurements and investigations of local EFs must be conducted.

The government of China has released standards to control the emissions of NMVOCs that result from the exploitation and distribution of fossil fuels and several sources associated with solvent use. Under current regulations, emissions of NMVOCs are projected to increase by 27% over the 2010 level by 2030, with emission reductions in the transportation and residential sectors. The enforcement of energy-saving policies and the implementation of end-of-pipe control measures would likely reduce the emissions of NMVOCs by 16% and 26%, respectively, in 2030 compared to the baseline scenario [8].

NH_3

NH_3 can lead to the formation of secondary fine particulates and has impacts on ecosystems. Huang *et al.* [238] developed a high-resolution inventory of NH_3 emissions for 2006 using a process-based model that represents EFs on a grid; these EFs are parameterized based on multiple factors, such as temperature and soil properties. Following the same framework, Kang *et al.* [240] compiled a long-term NH_3 emission inventory from 1980 to 2012. NH_3 emissions in China are estimated to have increased from 10.1 Tg in 2000 to 10.7 Tg in 2005; they then decreased to 9.3 Tg in 2012. The good agreement of the bottom-up emission estimates with the top-down inversion results [244] confirms the reliability and accuracy of these data.

In China, NH_3 emissions are dominated by livestock manure and the application of synthetic fertilizer and account for 80–90% of the total emissions. Livestock manure is the largest contributor, with proportions of approximately 50%. From 2000 to 2005, the emissions of livestock manure increased by 0.81 Tg (15%), leading to a rapid rise in total emissions [240]. Due to the reduced numbers of beef cattle and sheep, as well as promotion of the intensive rearing system, livestock emissions decreased by 18% from 2005 to 2012. The application of synthetic fertilization is responsible for 30–43% of the total emissions. From 2000 to 2012, the emissions from this source decreased from 3.79 to 2.81 Tg, which can be attributed to the substitution of urea for highly volatile ammonium bicarbonate (ABC).

The estimated total NH_3 emissions agree well among the different inventories, but variations by sector still exist, as shown in Kang *et al.* [240]. Additional local field measurements are needed to reduce the uncertainties in EFs and thus those of emission estimates.

PM

We present the changes in emissions of primary PM_{10}, $PM_{2.5}$, BC and OC in this subsection. PM degrades air quality and visibility, affects the climate system through increasing the radiative forcing and damages human health. Lei *et al.* [34] quantified the historical emissions of PM components using a technology-based framework and is an example of a pioneering native research study. The development of primary PM emission inventories for China has been a key topic of research that supports the assessment of haze-control policies since 2013.

PM_{10} and $PM_{2.5}$

The emissions of PM_{10} and $PM_{2.5}$ are estimated to have been 16 and 12 Tg in 2010, respectively, according to MEIC v1.2. The trends in the emissions of PM_{10} and $PM_{2.5}$ are similar among the different inventories. The emissions of PM_{10} and $PM_{2.5}$ increased by 15–17% and 15–20% from 2000 to 2005 [5,34] (MEIC v1.2) and decreased at rates of 10–17% and 6–15% from 2005 to 2010, respectively [6,8] (MEIC v1.2). Klimont *et al.* [5] arrived at an increasing trend in emissions for the latter period, likely due to different assumptions regarding technological evolution. Since 2012, the emissions of both PM_{10} and $PM_{2.5}$ have shown decreasing trends.

Downloaded from https://academic.oup.com/nsr/article-abstract/4/6/834/4775139
by guest
on 14 February 2018

Cement production and the combustion of biofuels in residential stoves are the largest emitters of $PM_{2.5}$, and these sources account for 11–33% and 24–28% of the total emissions during 2000 and 2015, respectively (MEIC v1.2). Power plants and transportation are minor contributors (less than 10%) to the total emissions. From 2000 to 2005, a boom in the production of iron and steel, cement and aluminium offset the effects of efficient PM control technologies, leading to the increase in emissions [34]. During 2005 to 2010, the use of highly effective PM abatement measures in the production of cement led to a reduction in emissions in this subsector of approximately 50%. The increase in large power plants equipped with efficient end-of-pipe dust collectors (e.g. electrostatic precipitators or fabric filters) reduced the EF of $PM_{2.5}$ by 46% from 2005 to 2010 [6]. Nevertheless, the emissions from iron and steel plants increased by 24–39% during the same period, due to the huge growth of steel production [6]. Local measurements of the PM EFs for the brick and coke industries, as well as coal and biofuel burning in the residential sector, are still limited.

In addition to end-of-pipe control measures, energy-saving policies could play a key role in reducing the emissions of PM_{10} and $PM_{2.5}$ by 2030. The effects of advanced energy-saving policies on $PM_{2.5}$ emissions (approximately 29% reduction, compared to the baseline scenario) exceed those of the planned end-of-pipe control measures (approximately 25% reduction) [8].

BC and OC

Emissions of BC and OC are estimated based on the mass ratio of each component in $PM_{2.5}$ for each source category. The measurements of the mass ratios for various sources before 2010 are summarized in Lei *et al.* [34]. BC emissions increased from 1.4 Tg in 2000 to 1.8 Tg in 2006, then showed a relatively flat and then a decreasing trend since 2006 (MEIC v1.2). Similarly, OC emissions increased from 2.7 Tg in 2000 to 3.5 Tg in 2005, remained at approximately 3.2 Tg from 2006 to 2012, then decreased to 2.5 Tg in 2015. The estimates of emissions reported by the different inventories show relatively good agreement, probably because they use similar EFs for sources for which few local measurements are available (e.g. brick and coke production).

BC and OC emissions are dominated by the residential consumption of biofuels, which accounts for 23–33% and 57–70% of the total, respectively. The significant increase between 2000 and 2005 occurred primarily due to the combustion of biofuels (+0.13 Tg of BC, +0.51 Tg of OC), followed by the coke industry (+0.09 Tg of BC, +0.11 Tg of OC) and the transportation sector (+0.04 Tg of BC, +0.02 Tg of OC) [34]. Since 2005, the sectoral distributions of both species have been relatively stable.

Toxic heavy metals. The development of emission inventories that are more complete in terms of the source categories and hazardous air pollutants are becoming increasingly important for protecting human health in the future. Quantitative assessments of the emissions and spatial distributions of toxic heavy metals, including Hg, As, Se, Pb, Cd, Cr, Ni, Sb, Mn, Co, Cu and Zn; the attribution of these emissions to particular sources; and policy controls on the releases of these metals from anthropogenic sources have been extensively studied in a series of papers [272–276]. The historical results for the period of 2000–12 show increases in the emissions of Hg, Cd, Sb, Cu and Zn that exceed a factor of two; increases in the emissions of As, Se, Cr, Ni, Mn and Co of 20–59% and a 29% reduction in Pb emissions reached approximately 526.9–22 319.6 Mg (varying among species) in 2012 [276]. Brake wear, which is the main source of hazardous metals from the transportation sector, should be considered in future work; no emission standard has been released that addresses this source of hazardous metals.

MODEL-READY EMISSION INVENTORY

Spatial allocation

In addition to the estimation of total emissions, gridded emissions are also needed for application in chemical transport models. Allocating emissions according to the geographic coordinates of emission sources is the most accurate method of generating gridded emissions. However, such information is not usually available, especially for mobile and areal emission sources, for which exact locations are unknown. Therefore, certain parameters that may represent the spatial distributions of emissions are employed in the gridding process; these parameters are referred to as spatial proxies.

After reviewing several global and regional emission inventories covering China, we find that the spatial proxies used in current inventories are usually shared among the different pollutant species; however, they differ among sectors. In the power sector, early studies used latitudes and longitudes to allocate the emissions from large-capacity power units, whereas population density was used for small power plants [1,2,12,22]. Recently, more detailed power plant databases have been developed, such as CARMA [37] and CPED [19], which contain

Downloaded from https://academic.oup.com/nsr/article-abstract/4/6/834/4775139
by guest
on 14 February 2018

more information on the locations of power emissions than was provided by previous work.

For the industrial sector, total population [1,12,13] or urban population [2] are most commonly used as spatial proxies, based on the assumption that such emissions are closely related to human activities. However, Geng *et al.* [284] have shown that this method may incorrectly allocate greater amounts of emissions to rural areas and underestimate urban emissions. Using county-level industrial GDP data as a constraint to map emissions from provinces to counties before gridding [36] could enhance the accuracy of estimated urban emissions and yield better model performance at the county level [284]. Recent studies have adopted large datasets indicating the locations of manufacturing facilities that produce products including coke, iron, steel and cement to enable the generation of high-resolution (e.g. $0.05^{\circ} \times 0.05^{\circ}$) and more accurate emission inventories [15,285,286].

In the transportation sector, pollutants are emitted from objects that follow trajectories; thus, road networks are frequently used to distribute on-road vehicle emissions [1,12] and ship lanes are used to apportion shipping emissions [1]. The hidden assumption in this method is that traffic volumes are homogeneous within provinces. To reduce the biases produced by this assumption, some studies have used county-level GDP [137] or county-level vehicle populations [16] as a first-pass spatial proxy to allocate emissions from provinces to counties before using the road networks. Zheng *et al.* [16] also utilized different types of road networks (e.g. highways and national, provincial and county roads); the total VKT data were used to weight each road type to further improve the allocation accuracy.

For the residential sector, total and rural population density have been widely used for gridding [2,36], though large uncertainties persist.

Review of the spatial proxies used in the Chinese emission inventory shows that the selection of spatial proxies is primarily empirical and work has been carried out to assess the uncertainties in gridded emissions introduced by the use of spatial proxies [284,285]. Additional efforts are needed in the future to improve the spatial distribution of emissions.

Temporal variation

Temporally resolved emissions with an hourly resolution are typically required by regional chemical transport models (CTMs). The temporal variations in emissions are largely driven by the activity strength or emission characteristics of their sources. For the open burning of agricultural waste, fire data derived from MODIS are used to estimate emissions at daily resolution [238]. The monthly emissions due to other anthropogenic activities are estimated by assigning the monthly profiles for each source category; further allocation to daily and hourly emissions is carried out based on the weekly and diurnal profiles, respectively. Emission processing systems that carry out temporal allocation have been proposed and validated using the Sparse Matrix Operator Kernel Emissions (SMOKE) model for China [287,288].

Monthly profiles by source are developed based on the monthly statistics of fuel consumption, industrial production or other relevant indicators [3,13,19,287]. In summary, for power plants, emissions are allocated to months based on monthly electricity generation. Industrial monthly profiles are derived from the yields of industrial products or industrial GDP for each month derived from statistical reports. For residential sources, monthly profiles are estimated from the stove operation time, according to ambient temperatures [1–3,13]. Zhu *et al.* [112] and Chen *et al.* [289] set up regression models to characterize the temporal variations of energy use in the residential sector based on temperature-related variables and socio-economic parameters. For agricultural activities, monthly emissions are estimated using monthly parameters, such as soil pH values and surface temperatures [238].

The available weekly and hourly profiles are restricted to specific regions (e.g. PRD) and limited source categories for which field investigations have been performed (e.g. urban and highway on-road vehicles) [290]. For the other sectors, the weekly and diurnal profiles were developed using working schedules, source characteristics, research reports and preliminary field measurements [287]. Information on the weekly and diurnal variations in each source is rarely available. Profiles are always shared among source categories that have similar temporal characteristics. Accurate databases of weekly and diurnal profiles covering complete source categories within different regions in China are needed.

Source profiles and chemical speciation

Speciation of NMVOCs

NMVOCs consist of a variety of chemical species that differ significantly in their chemical structures and reactivity in producing ozone and secondary organic aerosols (SOAs). In CTMs, NMVOCs are usually characterized by a specific chemical mechanism that represents theses differences. The

Downloaded from https://academic.oup.com/nsr/article-abstract/4/6/834/4775139
by guest
on 14 February 2018

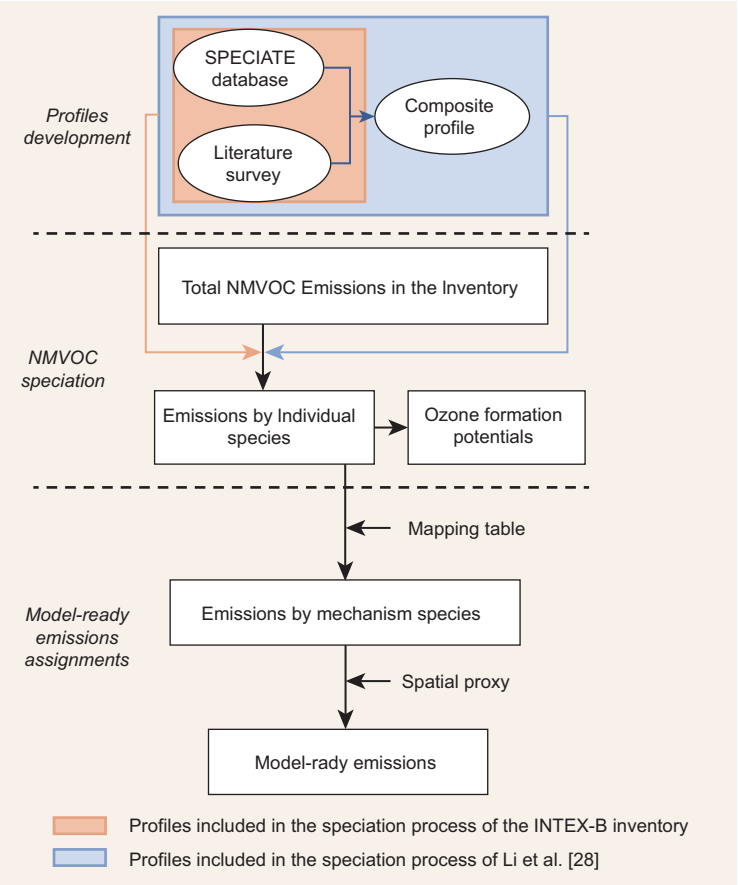

Figure 5. Schematic methodology of NMVOCs speciation (adapted from Li *et al.* [28]).

most commonly used mechanisms include the 1999 version of the State Air Pollution Research Center (SAPRC-99) [291] and its updated version SAPRC-07 [292]; Carbon Bond Mechanism version IV (CB-IV) [293], Carbon Bond Mechanism version Z (CBMZ) [294] and CB05 [295]; the Regional Acid Deposition Model chemical mechanism (RADM2) [296]; and the Regional Atmospheric Chemistry Mechanism (RACM and RACM2) [297,298]. Individual species are lumped together based on similarities in their carbon bond types (CB-IV, CB05, CBMZ) or functional groups (SAPRC-99, SAPRC-07, RADM2, RACM2). Therefore, NMVOC emissions should be speciated into the specific chemical mechanism configured in CTM.

Zhang *et al.* [2] developed a speciated NMVOC emission inventory for a variety of chemical mechanisms (e.g. SAPRC-99, CB05, RADM2) using an explicit speciation assignment approach. Following the same method, a unified framework for NMVOC speciation with an updated composite profile development method has been proposed by Li *et al.* [28] to generate model-ready emissions of multiple chemical mechanisms for Asia, as shown in Fig. 5. First, composite profiles were developed in this work by averaging the profiles of the same source category to reduce the potential uncertainty associated with the selection of a single-source profile. The emissions of individual species were then developed using the composite profile for each source. Second, the individual species were lumped to different chemical mechanisms using the corresponding species mapping tables. Li *et al.* [28] pointed out that the OVOCs (oxygenated VOCs) were missing from some locally measured profiles due to improper sampling and analysis methods, especially for biofuel combustion and diesel engine operation. A framework for correcting the fractions of OVOCs in composite profiles was also developed by Li *et al.* [28].

Source profiles are the most important source of uncertainties in the speciation of NMVOCs. Mo *et al.* [299] compiled a source profile database for hydrocarbons and OVOCs in China by summarizing recent available profiles. In the last several decades, increasing numbers of local profiles have been measured that cover important sources, including residential fuel combustion [114,126,179,299], solvent use [179,300,301], the paint industry [302], the petrochemical industry [179,303,304], the coking industry [305], on-road vehicles [179,299,306–313] and fuel evaporation [180]. Recent profiles have included OVOCs in their measurements, thus making the results more complete and reliable.

The emission characteristics of NMVOCs produced by various sources have been presented by numerous studies [10,21,28,100,169,236,299,237,314]. The emission distributions of chemical species are relatively consistent among investigations. For China as a whole, alkanes, alkenes, aromatics and OVOCs are the main contributors to the total emissions, and these classes of compounds have mass fractions of 24–30%, 19–28%, 15–30% and 12–18%, respectively. OVOCs made up 54% of the total VOCs within heavy-duty diesel vehicle exhaust and 12–46% of those produced by residential biofuel and coal burning, demonstrating the importance of OVOCs for combustion-related sources. Ethene, xylene, toluene, propene, 2-methyl-2-butene, 1,2,4-trimethylbenzene, butene and OVOC species (formaldehyde and glyoxal) are the main contributors to ozone formation that are produced by anthropogenic sources [21,28].

Measurements of local industrial profiles are still insufficient. Additional reliable domestic profiles for industrial facilities (e.g. chemical plants, iron and steel plants and oil refineries) and for both stack and fugitive sources are needed. Apart from non-methane hydrocarbons, OVOCs and halocarbons should be sampled and analysed in profile measurements. Source profiles are better reported in the absolute mass (e.g. g/kg) instead of mass fraction (%) because the latter may be highly uncertain, due to

Downloaded from https://academic.oup.com/nsr/article-abstract/4/6/834/4775139
by guest
on 14 February 2018

the incompleteness of the list of species measured. The EFs primarily used in emission inventories are for non-methane hydrocarbons, leading to underestimates in total VOC emissions by up to 30%, due to the omission of OVOCs [299]. The EFs based on source profiles that include OVOC measurements must be revised to improve the accuracy of emission estimates.

Speciation of $PM_{2.5}$

The composition of primary $PM_{2.5}$, including BC, OC, sulphate, nitrate and other trace elements, play key roles in haze formation and climate change. In CTMs, PM is speciated into over 10 chemical species in the updated aerosol modules (such as AERO6) used in regional models, providing a basis for further simulations of the partitioning between gases and aerosols, SOA formation, aerosol ageing and other processes [315]. BC and OC are always inventoried, together with $PM_{2.5}$, whereas PM speciation is required to estimate the emissions of other species for application in CTMs.

The framework used in PM speciation mainly follows that used with NMVOCs. According to the source profiles for $PM_{2.5}$ for each source category, $PM_{2.5}$ is first speciated into various components and then mapped to the model-compatible species. Reff *et al.* [316] developed the first speciated $PM_{2.5}$ emission inventory with 37 trace elements based on the US National Emissions Inventory and the US SPECIATE profile database (available at https://www.epa.gov/air-emissions-modeling/speciate-version-45-through-40). Compared to the speciation of NMVOCs, research on the speciation of PM in China is still lagging. Fu *et al.* [23] speciated $PM_{2.5}$ into 18 species using available local source profiles from the YRD region. The covered species include EC, OC, sulphate, nitrate, H_2O, Na, Cl, NH_4^+, non-carbon organic matter, Al, Ca, Fe, Si, Ti, Mg, K, Mn and others. Nationwide model-ready emissions with PM speciation are still lacking.

Reliable source profiles of $PM_{2.5}$ are essential to the speciation process. Several local source profiles have been measured in China [23]; these profiles cover power plants [317,318], coal-fired boilers [319], industrial combustion [95,320], residential coal combustion [116,117], biomass burning [321], vehicles [322,323], cement production [324], iron and steel production [325] and coking [326]. The USA-based SPECIATE database can supplement the sources that are lacking in the local profiles. Given the differences in the composition of PM between China and Western countries that may occur due to differences in fuel quality, technology and control policies, more measurements and investigations of local source profiles of various sources for PM are needed.

SUMMARY OF UNCERTAINTIES AND LIMITATIONS

The uncertainty ranges of emission estimates are calculated through the propagation of error [1,13] or the Monte Carlo approach [6,103,327]. Table 10 presents the emission uncertainties estimated by different studies in China. The uncertainties in emissions by sector were also estimated by Zhao *et al.* [6] using the Monte Carlo framework. The estimated emissions of SO_2 and NO_x are found to have low uncertainties of –15–26% and –15–35%, respectively ([6], 95% CIs). A moderate uncertainty range is assigned to CO (–18–42%). The uncertainties in the emissions of primary aerosols (PM_{10}, $PM_{2.5}$, BC, OC) are much higher than those of the gaseous species, due to the highly uncertain contributions from the residential sector. The EFs are the main contributing parameters to the final emission uncertainties [6]. As indicated in the previous sections, the current limitations of emission estimation by sectors are summarized as follows.

Power plants: Local measurements of PM EFs are still limited, compared to SO_2 and NO_x, leading to relatively high uncertainties.

Industry: Very few local measurements of EFs for industrial boilers can be found. The consumption of fuel by industrial boilers is still highly uncertain. There are very large gaps in the local EFs for NMVOCs for most industrial processes, especially those associated with oil refineries, carbon black production and the chemical industry.

Residential: EFs show large variations among different measurements. The official statistics that describe the amounts of coal and biofuel consumed in residential stoves are highly uncertain. Both fuel consumption and the relevant EFs are assigned high uncertainties, due to the lack of reliable underlying local data.

Transportation: Current EFs of on-road vehicles are calculated based on models developed for Western countries, such as the USA-developed IVE and MOVES models. Most existing EF measurements were taken in the megacities, reducing their representativeness for producing national emission estimates. Provincial-scale and national-scale surveys for determining vehicle activities are still limited. Few measurements or surveys have been conducted for off-road engines, leading to high uncertainties in this subsector.

Solvent use: Investigations into the amounts of solvent used are limited. Real-world measurements of EFs are lacking for most emission sources associated with solvent use.

Agriculture: Local measurements of EFs for NH_3 are rare.

Downloaded from https://academic.oup.com/nsr/article-abstract/4/6/834/4775139
by guest
on 14 February 2018

Table 10. Uncertainties of emission estimates (95% confidence intervals, unit: %).

SO_2	NO_x	CO	NMVOC	NH_3	PM_{10}	$PM_{2.5}$	BC	OC	Year	References
±12	±31	±70	±68		±132	±130	±208	±258	2006	Zhang *et al.* [2]
					±91	±107	±187	±229	2005	Lei *et al.* [34]
−14–13	−13–37				−14–45	−17–54	−25–136	−40–121	2005	Zhao *et al.* [103]
−16–17							−41–80	−44–92	2010	Lu *et al.* [36]
±31	±37	±86	±78	±153	±114	±133	±176	±271	2008	Kurokawa *et al.* [13]
−15–26	−15–35	−18–42			−15–54	−15–63	−28–126	−42–114	2010	Zhao *et al.* [6]

In-field crop residue burning: The amounts of crop residues burned in fields and the corresponding EFs are still uncertain.

With regards to model-ready processing, the spatial and temporal allocations of emissions and the speciation of NMVOC/PM to model-configured mechanisms are investigated and summarized in the previous sections. Limitations include the lack of local measurements of temporal profiles (especially weekly and diurnal profiles), reliable spatial surrogates, and complete and reliable source profiles.

OUTLOOK

Based on the efforts made in previous studies, we have gained increased knowledge of the emission characteristics of large point sources, including power plants and cement plants, and other key sources including on-road vehicles, shipping, residential combustion and agriculture. More reliable statistics and survey-based data have been used to reduce the uncertainties in activity rates and technology distributions. Local EFs and source profiles covering various sources have been measured and reported. Independent validations including satellite-based and in-situ observations have been introduced for better constraints of emissions during the last decade.

Further efforts are required to improve the accuracy of emission inventories in China based on local data with high resolutions. Recent studies demonstrate that treating sources as point sources significantly improves the accuracy of both emission estimates and the inferred spatial distributions of emissions and thus model performance [285,328]. The development of inventory models that include greater numbers of point sources, such as cement plants, iron and steel plants and oil refineries, is anticipated to make key contributions. Given the gradual installation of continuous emission monitoring system (CEMS) in power plants in China, the accuracy of emission estimates can be further improved by including the real-time data. Integrating data describing traffic flow into the development of vehicular emission inventories should improve the accuracy of emission estimates significantly.

For sources that lack adequately detailed information, a mosaic of different statistical data may provide improved emission estimates [285]. Future work should focus on surveys of activity rates and measurements of EFs and source profiles in places where few such assessments have been carried out locally in China. Top-down validations based on ground and satellite observations continue to play important roles in improving the temporal and spatial characterizations contained within emission inventories in China.

Public access to emission inventories is another important issue to be addressed. As essential inputs to CTMs, public access to emission inventories and high transparency of such inventories can benefit both modellers and the inventory community. With wide application and independent validation, the uncertainties of emission inventories can be identified and further reduced. We encourage inventory developers to provide online access to emissions data grouped by sector and subsector, together with information on temporal variations, spatial distributions and chemical speciation (where possible) and the necessary documentation.

ACKNOWLEDGEMENTS

This work was supported by the National Key R&D program (2016YFC0201506), the National Natural Science Foundation of China (41625020, 41571130032 and 41571130035), and the National Basic Research Program of China (2014CB441301).

REFERENCES

1. Streets DG, Bond TC and Carmichael GR *et al.* An inventory of gaseous and primary aerosol emissions in Asia in the year 2000. *J Geophys Res* 2003; **108**: 8809.
2. Zhang Q, Streets DG and Carmichael GR *et al.* Asian emissions in 2006 for the NASA INTEX-B mission. *Atmos Chem Phys* 2009; **9**: 5131–53.
3. Li M, Zhang Q and Kurokawa JI *et al.* MIX: a mosaic Asian anthropogenic emission inventory under the international collaboration framework of the MICS-Asia and HTAP. *Atmos Chem Phys* 2017; **17**: 935–63.
4. Janssens-Maenhout G, Crippa M and Guizzardi D *et al.* HTAP˙v2.2: a mosaic of regional and global emission grid maps for 2008 and 2010 to study hemispheric transport of air pollution. *Atmos Chem Phys* 2015; **15**: 11411–32.

Downloaded from https://academic.oup.com/nsr/article-abstract/4/6/834/4775139
by guest
on 14 February 2018

5. Klimont Z, Kupiainen K and Heyes C *et al.* Global anthropogenic emissions of particulate matter including black carbon. *Atmos Chem Phys* 2017; **17**: 8681–723.
6. Zhao Y, Zhang J and Nielsen CP. The effects of recent control policies on trends in emissions of anthropogenic atmospheric pollutants and CO_2 in China. *Atmos Chem Phys* 2013; **13**: 487–508.
7. Zhao Y, Zhang J and Nielsen CP. The effects of energy paths and emission controls and standards on future trends in China's emissions of primary air pollutants. *Atmos Chem Phys* 2014; **14**: 8849–68.
8. Wang S, Zhao B and Cai SY *et al.* Emission trends and mitigation options for air pollutants in East Asia. *Atmos Chem Phys* 2014; **14**: 6571–603.
9. Kato N and Akimoto H. Anthropogenic emissions of SO_2 and NO_x in Asia: emission inventories. *Atmospheric Environment Part A General Topics* 1992; **26**: 2997–3017.
10. Klimont Z, Streets DG and Gupta S *et al.* Anthropogenic emissions of non-methane volatile organic compounds in China. *Atmos Environ* 2002; **36**: 1309–22.
11. Bond TC, Bhardwaj E and Dong R *et al.* Historical emissions of black and organic carbon aerosol from energy-related combustion, 1850–2000. *Global Biogeochem Cycles* 2007; **21**: GB2018.
12. Ohara T, Akimoto H and Kurokawa J *et al.* An Asian emission inventory of anthropogenic emission sources for the period 1980–2020. *Atmos Chem Phys* 2007; **7**: 4419–44.
13. Kurokawa J, Ohara T and Morikawa T *et al.* Emissions of air pollutants and greenhouse gases over Asian regions during 2000–2008: Regional Emission inventory in ASia (REAS) version 2. *Atmos Chem Phys* 2013; **13**: 11019–58.
14. Zhao Y, Wang S and Duan L *et al.* Primary air pollutant emissions of coal-fired power plants in China: current status and future prediction. *Atmos Environ* 2008; **42**: 8442–52.
15. Lei Y, Zhang Q and Nielsen C *et al.* An inventory of primary air pollutants and CO_2 emissions from cement production in China, 1990–2020. *Atmos Environ* 2011; **45**: 147–54.
16. Zheng B, Huo H and Zhang Q *et al.* High-resolution mapping of vehicle emissions in China in 2008. *Atmos Chem Phys* 2014; **14**: 9787–805.
17. Huang Y, Shen H and Chen H *et al.* Quantification of global primary emissions of PM2.5, PM10, and TSP from combustion and industrial process sources. *Environ Sci Technol* 2014; **48**: 13834–43.
18. Huang Y, Shen H and Chen Y *et al.* Global organic carbon emissions from primary sources from 1960 to 2009. *Atmos Environ* 2015; **122**: 505–12.
19. Liu F, Zhang Q and Tong D *et al.* High-resolution inventory of technologies, activities, and emissions of coal-fired power plants in China from 1990 to 2010. *Atmos Chem Phys* 2015; **15**: 13299–317.
20. Meng W, Zhong Q and Yun X *et al.* Improvement of a global high-resolution ammonia emission inventory for combustion and industrial sources with new data from the residential and transportation sectors. *Environ Sci Technol* 2017; **51**: 2821–9.
21. Zheng J, Shao M and Che W *et al.* Speciated VOC emission inventory and spatial patterns of ozone formation potential in the Pearl River Delta, China. *Environ Sci Technol* 2009; **43**: 8580–6.
22. Zhao B, Wang P and Ma JZ *et al.* A high-resolution emission inventory of primary pollutants for the Huabei region, China. *Atmos Chem Phys* 2012; **12**: 481–501.
23. Fu X, Wang S and Zhao B *et al.* Emission inventory of primary pollutants and chemical speciation in 2010 for the Yangtze River Delta region, China. *Atmos Environ* 2013; **70**: 39–50.
24. Yin S, Zheng J and Lu Q *et al.* A refined 2010-based VOC emission inventory and its improvement on modeling regional ozone in the Pearl River Delta Region, China. *Sci Total Environ* 2015; **514**: 426–38.
25. Guan D, Liu Z and Geng Y *et al.* The gigatonne gap in China's carbon dioxide inventories. *Nat Clim Change* 2012; **2**: 672–5.
26. Hong C, Zhang Q and He K *et al.* Variations of China's emission estimates: response to uncertainties in energy statistics. *Atmos Chem Phys* 2017; **17**: 1227–39.
27. Peng L, Zhang Q and Yao Z *et al.* Missing coal consumption from statistics: a survey-based solid fuel usage and emission inventory for rural residential sector in China. (By personal communication).
28. Li M, Zhang Q and Streets DG *et al.* Mapping Asian anthropogenic emissions of non-methane volatile organic compounds to multiple chemical mechanisms. *Atmos Chem Phys* 2014; **14**: 5617–38.
29. Klimont Z, Cofala J and Schöpp W *et al.* Projections of SO_2, NO_x, NH_3 and VOC emissions in East Asia up to 2030. *Water, Air, and Soil Pollution* 2001; **130**: 193–8.
30. Hao J, Tian H and Lu Y. Emission inventories of NO_x from commercial energy consumption in China, 1995—1998. *Environ Sci Technol* 2002; **36**: 552–60.
31. Zhang Q, Streets DG and He K *et al.* Major components of China's anthropogenic primary particulate emissions. *Environ Res Lett* 2007; **2**: 045027.
32. Zhang Q, Streets DG and He K *et al.* NO_x emission trends for China, 1995–2004: the view from the ground and the view from space. *J Geophys Res* 2007; **112**: D22306.
33. Klimont Z, Cofala J and Xing J *et al.* Projections of SO_2, NO_x and carbonaceous aerosols emissions in Asia. *Tellus B* 2009; **61**: 602–17.
34. Lei Y, Zhang Q and He KB *et al.* Primary anthropogenic aerosol emission trends for China, 1990–2005. *Atmos Chem Phys* 2011; **11**: 931–54.
35. Klimont Z, Smith SJ and Cofala J. The last decade of global anthropogenic sulfur dioxide: 2000–2011 emissions. *Environ Res Lett* 2013; **8**: 014003.
36. Lu Z, Zhang Q and Streets DG. Sulfur dioxide and primary carbonaceous aerosol emissions in China and India, 1996–2010. *Atmos Chem Phys* 2011; **11**: 9839–64.
37. Wheeler D and Ummel K. *Calculating CARMA: Global Estimation of CO_2 Emissions from the Power Sector*, Working Paper 145. : Center for Global Development. Washington, D.C., USA, 2008.
38. Oda T and Maksyutov S. A very high-resolution (1 km × 1 km) global fossil fuel CO_2 emission inventory derived using a point source database and satellite observations of nighttime lights. *Atmos Chem Phys* 2011; **11**: 543–56.
39. Wang R, Tao S and Ciais P *et al.* High-resolution mapping of combustion processes and implications for CO_2 emissions. *Atmos Chem Phys* 2013; **13**: 5189–203.
40. Zhao Y, Wang S and Duan L *et al.* Primary air pollutant emissions of coal-fired power plants in China: current status and future prediction. *Atmos Environ* 2008; **42**: 8442–52.
41. Wang SW, Zhang Q and Streets DG *et al.* Growth in NO_x emissions from power plants in China: bottom-up estimates and satellite observations. *Atmos Chem Phys* 2012; **12**: 4429–47.
42. Tian H, Liu K and Hao J *et al.* Nitrogen oxides emissions from thermal power plants in China: current status and future predictions. *Environ Sci Technol* 2013; **47**: 11350–7.
43. Chen L, Sun Y and Wu X *et al.* Unit-based emission inventory and uncertainty assessment of coal-fired power plants. *Atmos Environ* 2014; **99**: 527–35.
44. Lu Z, Streets DG and Zhang Q *et al.* Sulfur dioxide emissions in China and sulfur trends in East Asia since 2000. *Atmos Chem Phys* 2010; **10**: 6311–31.

Downloaded from https://academic.oup.com/nsr/article-abstract/4/6/834/4775139
by guest
on 14 February 2018

45. Li C, Zhang Q and Krotkov NA *et al.* Recent large reduction in sulfur dioxide emissions from Chinese power plants observed by the Ozone Monitoring Instrument. *Geophys Res Lett* 2010; **37**: L08807.
46. Xu Y, Williams RH and Socolow RH. China's rapid deployment of SO_2 scrubbers. *Energy Environ Sci* 2009; **2**: 459–65.
47. Xu Y. China's functioning market for sulfur dioxide scrubbing technologies. *Environ Sci Technol* 2011; **45**: 9161–7.
48. Yao W. Experiment on the SO_2 removal efficiency of wet scrubbers (in Chinese). *Environmental Protection* 1989; **2**: 11–13.
49. Xie Z. Wet dedusting, desulfurization and denitrification without using additives for coal-fired boilers (in Chinese). *China Environmental Protection Industry* 1995; **3**: 22–3.
50. SEPA. *Emission Standard of Air Pollutants for Thermal Power Plants: GB 13223–1996*. Beijing: China Environmental Science Press, 1996.
51. Klimont Z, Cofala J and Bertok I *et al. Modeling Particulate Emissions in Europe: A Framework to Estimate Reduction Potential and Control Costs*, Interim Report, IR-02-076. Laxenburg: International Institute for Applied Systems Analysis, 2002.
52. Amann M, Bertok I and Borken-Kleefeld J *et al.* Cost-effective control of air quality and greenhouse gases in Europe: Modeling and policy applications. *Environ Modell Softw* 2011; **26**: 1489–501.
53. Qian C. Study on air staged low NO_x emission combustion technology (in Chinese). *Shanghai Electricity* 2010; **1**: 38–40.
54. Cao D and Liu H. Study on NO_x emission control technology of boilers (in Chinese). *Water Conservancy & Electric Power Machinery* 2011; **33**: 69–72.
55. Zhu L. Modification of low nitrogen oxide combustion for 300MW coal-fired boiler (in Chinese). *Guangdong Electric Power* 2009; **22**: 64–7.
56. Wang X, Luan T and Cheng L. Experimental study on performance and NO_x emission of large coal-fired boilers (in Chinese). *Power Equipment* 2008; **6**: 467–72.
57. Yi HH, Hao JM and Duan L *et al.* Characteristics of inhalable particulate matter concentration and size distribution from power plants in China. *JAPCA J Air Waste MA* 2006; **56**: 1243–51.
58. Zhu F, Liu D and Wang S. Overview of NO_x emissions and control measures from thermal power plants (in Chinese). *Environmental Protection* 2009; **21**: 40–1.
59. Xie J, Zhang S and Xia Y. Analysis of performance and NO_x emission of 600MW boilers (in Chinese). *Dongfang Boiler* 2008; **3**: 12–6.
60. Wang X, Xin H and Luan T *et al.* Research and test on influence of boiler combustion adjusting on NO_x emission of 330MW unit (in Chinese). *Power Sys Eng* 2007; **23**: 7–10.
61. Bi Y and Chen G. Countermeasures and suggestions for controlling NO_x emission of utility boilers (in Chinese). *Electricity* 2004; **15**: 41–5.
62. Tian H. *Studies on present and future emissions of nitrogen oxides and its comprehensive control policies in China (in Chinese). Ph.D. Dissertation.* Tsinghua University 2003.
63. Zhu F. *Study on NO_x Emission Reduction Potential and Gross Control Measures of Thermal Power Plants in China (in Chinese).* Nanjing: State Power Environmental Protection Research Institute, 2011.
64. Zhu F, Wang S and Zheng Y. NO_x emitting current situation and forecast from thermal power plants and countermeasures (in Chinese). *Energy Environ Prot* 2004; **18**: 1–5.
65. Feng M and Yan H. Research on the concentration value conversion of NO_x in the flue gas from thermal power plants (in Chinese). *Shanxi Eletric Power* 2007; **143**: 14–20.
66. Zhao Y, Wang S and Nielsen CP *et al.* Establishment of a database of emission factors for atmospheric pollutants from Chinese coal-fired power plants. *Atmos Environ* 2010; **44**: 1515–23.
67. Huang W, Luo ZY and Xu H *et al.* Research on distribution of aerosol and PAHs in power plant stack (in Chinese). *Energ Eng* 2003; **2**: 29–32.
68. Liu JZ, Fan HY and Zhou JH *et al.* Experimental studies on the emissions of PM10 and PM2.5 from coal-fired boiler (in Chinese). *Proceedings of the CSEE* 2003; **23**: 145–9.
69. Zhao B, Wang SX and Liu H *et al.* NO_x emissions in China: historical trends and future perspectives. *Atmos Chem Phys* 2013; **13**: 9869–97.
70. Hua S, Tian H and Wang K *et al.* Atmospheric emission inventory of hazardous air pollutants from China's cement plants: temporal trends, spatial variation characteristics and scenario projections. *Atmos Environ* 2016; **128**: 1–9.
71. Wang K, Tian H and Hua S *et al.* A comprehensive emission inventory of multiple air pollutants from iron and steel industry in China: temporal trends and spatial variation characteristics. *Sci Total Environ* 2016; **559**: 7–14.
72. Wang X, Yan L and Lei Y *et al.* Estimation of primary particulate emissions from iron and steel industry in China (in Chinese). *Acta Scientiae Circumstantiae* 2016; **36**: 3033–9.
73. US Geological Survey (USGS). *Mineral Commodity Summaries 2014*. Washington: United States Government Printing Office, 2014.
74. Zhang Q, Klimont Z and Streets D *et al.* An anthropogenic PM emission model for China and emission inventory for the year 2001 (in Chinese). 2006; **16**: 223–31.
75. Zhang C, Wang S and Zhao Y *et al.* Current status and future prospects of anthropogenic particulate matter emissions in China (in Chinese). *Environ Sci* 2009; **30**: 1881–7.
76. Lei Y, He K and Zhang Q *et al.* Technology-based emission inventory of particulate matters (PM) from cement industry (in Chinese). *Huan Jing Ke Xue* 2008; **29**: 2366–71.
77. Woo J-H, Baek JM and Kim JW *et al.* Development of a multi-resolution emission inventory and its impact on sulfur distribution for Northeast Asia. *Water, Air, and Soil Pollution* 2003; **148**: 259–78.
78. Liu H. Control of SO_2 from cement kiln systems (in Chinese). *China Cement* 2006; **11**: 74–7.
79. Wu H. NOx emission limits of policy analysis in cement industry (in Chinese). *Sichuan Cement* 2012; **a01**: 36–8.
80. Yuan W, Chen Z and Cao W *et al.* Implementing policy for new pollutants emission standards in cement industry (in Chinese). *Jiangsu Building Materials* 2005; **2**: 16–27.
81. Ren C, Jiang M and Zou L *et al.* Study on feasible emission control level of air pollutions for cement industry (in Chinese). *Environ Sci* 2014; **35**: 3632–8.
82. Guo B and Tian W. Selection of examining methods for total emission control of SO_2 and NO_x in cement industry (in Chinese). *Shanghai Environ Sci* 2012; **31**: 38–46.
83. Liu X. emission characteristics of gaseous pollutants (SO_2, NO_x and fluoride) in cement industry (in Chinese). *Environ Sustain Development* 2016; **41**: 239–40.
84. Chen L, Liu S and Zhao W *et al.* The emission and control of NO_x for new dry cement kilns (in Chinese). *Air Pollution Prevention and Control* 2016; **38**: 40–3.
85. Su D, Gao D and Ye H. Harmful gases pollution and its remedy in cement kiln (in Chinese). *Chongqing Environmental Science* 1998; **20**: 20–3.
86. Ding X, Wang Y and Yu X *et al.* Air pollutants emission and management research in China's cement industry (in Chinese). *China Cement* 2010; **11**: 47–50.

Downloaded from https://academic.oup.com/nsr/article-abstract/4/6/834/4775139
by guest
on 14 February 2018

87. Li L. In the environment statistical work of cement industry nitrogen oxide and sulfur dioxide emissions factors of cement industry in the environment statistical work (in Chinese). *Statistics and Consulting* 2007; **5**: 29–30.
88. Wang Y, Xue Z and Chai F *et al.* Estimation of air pollutants emissions of cement industry in China (in Chinese). *Res Environ Sci* 2008; **21**: 207–12.
89. Wang S, Xing J and Chatani S *et al.* Verification of anthropogenic emissions of China by satellite and ground observations. *Atmos Environ* 2011; **45**: 6347–58.
90. Chen W, Hong J and Xu C. Pollutants generated by cement production in China, their impacts, and the potential for environmental improvement. *J Clean Prod* 2015; **103**: 61–9.
91. Wu X, Zhao L and Zhang Y *et al.* Primary air pollutant emissions and future prediction of iron and steel industry in China. *Aerosol Air Qual Res* 2015; **15**: 1422–32.
92. Ge S, Bai Z and Liu W *et al.* Boiler briquette coal versus raw coal: Part I—Stack gas emissions. *JAPCA J Air Waste MA* 2001; **51**: 524–33.
93. Zhang Y, Schauer JJ and Zhang Y *et al.* Characteristics of particulate carbon emissions from real-world Chinese coal combustion. *Environ Sci Technol* 2008; **42**: 5068–73.
94. Li C, Li X-H and Duan L *et al.* Emission characteristics of PM10 from coal-fired industrial boiler (in Chinese). *Huan Jing Ke Xue* 2009; **30**: 650–5.
95. Wang S, Zhao X-J and Li X-H *et al.* Emission characteristics of fine particles from grate firing boilers (in Chinese). *Huan Jing Ke Xue* 2009; **30**: 963–8.
96. UNEP. *A Review of Air Pollution Control in Beijing 1998–2013*. Nairobi: United Nations Environment Programme (UNEP), 2016.
97. UNEP. *UNEP Environmental Assessment: EXPO 2010 Shanghai, China*. Nairobi: United Nations Environment Programme (UNEP), 2010.
98. Qiu K, Yang L and Lin J *et al.* Historical industrial emissions of non-methane volatile organic compounds in China for the period of 1980–2010. *Atmos Environ* 2014; **86**: 102–12.
99. Wu X, Huang W and Zhang Y *et al.* Characteristics and uncertainty of industrial VOCs emissions in China. *Aerosol Air Qual Res* 2015; **15**: 1045–58.
100. Wei W, Wang S and Chatani S *et al.* Emission and speciation of non-methane volatile organic compounds from anthropogenic sources in China. *Atmos Environ* 2008; **42**: 4976–88.
101. Bo Y, Cai H and Xie SD. Spatial and temporal variation of historical anthropogenic NMVOCs emission inventories in China. *Atmos Chem Phys* 2008; **8**: 7297–316.
102. Wu R, Bo Y and Li J *et al.* Method to establish the emission inventory of anthropogenic volatile organic compounds in China and its application in the period 2008–2012. *Atmos Environ* 2016; **127**: 244–54.
103. Zhao Y, Nielsen CP and Lei Y *et al.* Quantifying the uncertainties of a bottom-up emission inventory of anthropogenic atmospheric pollutants in China. *Atmos Chem Phys* 2011; **11**: 2295–308.
104. Yang X, Jiang Y and Yang M *et al.* Energy and environment in Chinese rural housing: current status and future perspective. *Front Energy Power Eng China* 2010; **4**: 35–46.
105. Duan X, Jiang Y and Wang B *et al.* Household fuel use for cooking and heating in China: results from the first Chinese Environmental Exposure-Related Human Activity Patterns Survey (CEERHAPS). *Appl Energ* 2014; **136**: 692–703.
106. Liu W, Spaargaren G and Heerink N *et al.* Energy consumption practices of rural households in north China: basic characteristics and potential for low carbon development. *Energ Policy* 2013; **55**: 128–38.
107. Sun E, Wang L and Lai X *et al.* Impacts and solutions of northern China winter rural heating on PM2.5. *Environ Sci Manag* 2013; **38**: 90–3.
108. Zhang Y, Jiang J and Ye J *et al.* Testing the evolution of crude oil market efficiency: data have the conn. *Energ Policy* 2014; **36**: 39–52.
109. Zhao W, Xu Q and Li L *et al.* Estimation of air pollutant emissions from coal burning in the semi-rural areas of Beijing Plain (in Chinese). *Res Environ Sci* 2015; **28**: 869–76.
110. Zhi GR, Yang JC and Tao Z *et al.* Rural household coal use survey, emission estimation and policy implications (in Chinese). *Res Environ Sci* 2015; **28**: 1179–85.
111. Cheng M, Zhi G and Tang W *et al.* Air pollutant emission from the underestimated households' coal consumption source in China. *Sci Total Environ* 2017; **580**: 641–50.
112. Zhu D, Tao S and Wang R *et al.* Temporal and spatial trends of residential energy consumption and air pollutant emissions in China. *Appl Energ* 2013; **106**: 17–24.
113. Zhang J, Smith KR and Ma Y *et al.* Greenhouse gases and other airborne pollutants from household stoves in China: a database for emission factors. *Atmos Environ* 2000; **34**: 4537–49.
114. Tsai SM, Zhang J and Smith KR *et al.* Characterization of non-methane hydrocarbons emitted from various cookstoves used in China. *Environ Sci Technol* 2003; **37**: 2869–77.
115. Chen Y, Sheng G and Bi X *et al.* Emission factors for carbonaceous particles and polycyclic aromatic hydrocarbons from residential coal combustion in China. *Environ Sci Technol* 2005; **39**: 1861–7.
116. Chen Y, Zhi G and Feng Y *et al.* Measurements of emission factors for primary carbonaceous particles from residential raw-coal combustion in China. *Geophys Res Lett* 2006; **33**: L20815.
117. Zhi G, Chen Y and Feng Y *et al.* Emission characteristics of carbonaceous particles from various residential coal-stoves in China. *Environ Sci Technol* 2008; **42**: 3310–5.
118. Li X, Wang S and Duan L *et al.* Carbonaceous aerosol emissions from household biofuel combustion in China. *Environ Sci Technol* 2009; **43**: 6076–81.
119. Shen G, Yang Y and Wang W *et al.* Emission factors of particulate matter and elemental carbon for crop residues and coals burned in typical household stoves in China. *Environ Sci Technol* 2010; **44**: 7157–62.
120. Shen G, Wei S and Wei W *et al.* Emission factors, size distributions, and emission inventories of carbonaceous particulate matter from residential wood combustion in rural China. *Environ Sci Technol* 2012; **46**: 4207–14.
121. Shen G, Tao S and Wei S *et al.* Field measurement of emission factors of PM, EC, OC, parent, nitro-, and oxy- polycyclic aromatic hydrocarbons for residential briquette, coal cake, and wood in rural Shanxi, China. *Environ Sci Technol* 2013; **47**: 2998–3005.
122. Shen G, Xue M and Wei S *et al.* Influence of fuel moisture, charge size, feeding rate and air ventilation conditions on the emissions of PM, OC, EC, parent PAHs, and their derivatives from residential wood combustion. *J Environ Sci* 2013; **25**: 1808–16.
123. Shen G, Chen Y and Xue C *et al.* Pollutant emissions from improved coal- and wood-fuelled cookstoves in rural households. *Environ Sci Technol* 2015; **49**: 6590–8.
124. Ge S, Xu X and Chow JC *et al.* Emissions of air pollutants from household stoves: honeycomb coal versus coal cake. *Environ Sci Technol* 2004; **38**: 4612–8.
125. Chen Y, Zhi G and Feng Y *et al.* Measurements of black and organic carbon emission factors for household coal combustion in China: implication for emission reduction. *Environ Sci Technol* 2009; **43**: 9495–500.
126. Wang S, Wei W and Du L *et al.* Characteristics of gaseous pollutants from biofuel-stoves in rural China. *Atmos Environ* 2009; **43**: 4148–54.
127. Wei W, Zhang W and Hu D *et al.* Emissions of carbon monoxide and carbon dioxide from uncompressed and pelletized biomass fuel burning in typical household stoves in China. *Atmos Environ* 2012; **56**: 136–42.

Downloaded from https://academic.oup.com/nsr/article-abstract/4/6/834/4775139
by guest
on 14 February 2018

128. Kelly FJ and Zhu T. Transport solutions for cleaner air. *Science* 2016; **352**: 934–6.
129. Wang F, Lin T and Feng J *et al.* Source apportionment of polycyclic aromatic hydrocarbons in PM2.5 using positive matrix factorization modeling in Shanghai, China. *Environmental Science: Processes & Impacts* 2015; **17**: 197–205.
130. Wang G, Cheng S and Li J *et al.* Source apportionment and seasonal variation of PM2.5 carbonaceous aerosol in the Beijing-Tianjin-Hebei Region of China. *Environ Monit Assess* 2015; **187**: 143.
131. Cui H, Chen W and Dai W *et al.* Source apportionment of PM2.5 in Guangzhou combining observation data analysis and chemical transport model simulation. *Atmos Environ* 2015; **116**: 262–71.
132. Guo Z, Shi L and Chen S *et al.* Sulfur isotopic fractionation and source appointment of PM2.5 in Nanjing region around the second session of the Youth Olympic Games. *Atmos Res* 2016; **174**: 9–17.
133. Cuddihy RG, Griffith WC and McClellan RO. Health risks from light-duty diesel vehicles. *Environ Sci Technol* 1984; **18**: 14A–21A.
134. Crump KS, Van Landingham C and Moolgavkar SH *et al.* Reanalysis of the DEMS nested case-control study of lung cancer and diesel exhaust: suitability for quantitative risk assessment. *Risk Anal* 2015; **35**: 676–700.
135. Anenberg SC, Miller J and Minjares R *et al.* Impacts and mitigation of excess diesel-related NO_x emissions in 11 major vehicle markets. *Nature* 2017; **545**: 467–71.
136. Walsh M. Global trends in motor vehicle use and emissions. *Annu Rev Energy* 1990; **15**: 217–43.
137. Cai H and Xie S. Estimation of vehicular emission inventories in China from 1980 to 2005. *Atmos Environ* 2007; **41**: 8963–79.
138. Cai H and Xie SD. Tempo-spatial variation of emission inventories of speciated volatile organic compounds from on-road vehicles in China. *Atmos Chem Phys* 2009; **9**: 6983–7002.
139. Huo H, Zhang Q and He K *et al.* High-resolution vehicular emission inventory using a link-based method: a case study of light-duty vehicles in Beijing. *Environ Sci Technol* 2009; **43**: 2394–9.
140. Wang H, Fu L and Zhou Y *et al.* Trends in vehicular emissions in China's mega cities from 1995 to 2005. *Environ Pollut* 2010; **158**: 394–400.
141. Wu Y, Wang R and Zhou Y *et al.* On-road vehicle emission control in Beijing: past, present, and future. *Environ Sci Technol* 2011; **45**: 147–53.
142. Wu Y, Zhang S and Hao J *et al.* On-road vehicle emissions and their control in China: a review and outlook. *Sci Total Environ* 2017; **574**: 332–49.
143. Lang J, Cheng S and Zhou Y *et al.* Air pollutant emissions from on-road vehicles in China, 1999–2011. *Sci Total Environ* 2014; **496**: 1–10.
144. Yang X, Liu H and Man HY *et al.* Characterization of road freight transportation and its impact on the national emission inventory in China. *Atmos Chem Phys* 2015; **15**: 2105–18.
145. Zhou Y, Shuiyuan C and Lang J *et al.* A comprehensive ammonia emission inventory with high-resolution and its evaluation in the Beijing–Tianjin–Hebei (BTH) region, China. *Atmos Environ* 2015; **106**: 305–17.
146. Sun S, Jiang W and Gao W. Vehicle emission trends and spatial distribution in Shandong province, China, from 2000 to 2014. *Atmos Environ* 2016; **147**: 190–9.
147. Zhang S, Wu Y and Huang R *et al.* High-resolution simulation of link-level vehicle emissions and concentrations for air pollutants in a traffic-populated eastern Asian city. *Atmos Chem Phys* 2016; **16**: 9965–81
148. Hao J, He D and Wu Y *et al.* A study of the emission and concentration distribution of vehicular pollutants in the urban area of Beijing. *Atmos Environ* 2000; **34**: 453–65.
149. Fu L, Hao J and He D *et al.* Assessment of vehicular pollution in China. *JAPCA J Air Waste MA* 2001; **51**: 658–68.
150. Liu H, He K and Lents JM *et al.* Characteristics of diesel truck emission in China based on portable emissions measurement systems. *Environ Sci Technol* 2009; **43**: 9507–11.
151. Zhang S, Wu Y and Wu X *et al.* Historic and future trends of vehicle emissions in Beijing, 1998–2020: a policy assessment for the most stringent vehicle emission control program in China. *Atmos Environ* 2014; **89**: 216–29.
152. Wang G, Cheng S and Lang J *et al.* On-board measurements of gaseous pollutant emission characteristics under real driving conditions from light-duty diesel vehicles in Chinese cities. *J Environ Sci* 2016; **46**: 28–37.
153. Huo H, Yao Z and Zhang Y *et al.* On-board measurements of emissions from light-duty gasoline vehicles in three mega-cities of China. *Atmos Environ* 2012; **49**: 371–7.
154. Fu M, Ge Y and Wang X *et al.* NO_x emissions from Euro IV busses with SCR systems associated with urban, suburban and freeway driving patterns. *Sci Total Environ* 2013; **452**: 222–6.
155. Huang C, Lou D and Hu Z *et al.* A PEMS study of the emissions of gaseous pollutants and ultrafine particles from gasoline- and diesel-fueled vehicles. *Atmos Environ* 2013; **77**: 703–10.
156. Wang X, Yin H and Ge Y *et al.* On-vehicle emission measurement of a light-duty diesel van at various speeds at high altitude. *Atmos Environ* 2013; **81**: 263–9.
157. Guo J, Ge Y and Hao L *et al.* On-road measurement of regulated pollutants from diesel and CNG buses with urea selective catalytic reduction systems. *Atmos Environ* 2014; **99**: 1–9.
158. Shen X, Yao Z and Huo H *et al.* PM2.5 emissions from light-duty gasoline vehicles in Beijing, China. *Sci Total Environ* 2014; **487**: 521–7.
159. Shen X, Yao Z and Zhang Q *et al.* Development of database of real-world diesel vehicle emission factors for China. *J Environ Sci* 2015; **31**: 209–20.
160. Zhang Y, Yao Z and Shen X *et al.* Chemical characterization of PM 2.5 emitted from on-road heavy-duty diesel trucks in China. *Atmos Environ* 2015; **122**: 885–91.
161. Liu J, Ge Y and Wang X *et al.* On-board measurement of particle numbers and their size distribution from a light-duty diesel vehicle: Influences of VSP and altitude. *J Environ Sci* 2017; **57**: 238–48.
162. Xie C-q and Parker D. A social psychological approach to driving violations in two Chinese cities. *Transport Res F-Traf* 2002; **5**: 293–308.
163. Liu H, He K and Wang Q *et al.* Comparison of Vehicle Activity and Emission Inventory between Beijing and Shanghai. *JAPCA J Air Waste MA* 2007; **57**: 1172–7.
164. Liu H, Man H and Cui H *et al.* An updated emission inventory of vehicular VOCs and IVOCs in China. *Atmos Chem Phys* 2017; **17**: 12709–24.
165. Liu H, He K and Barth M. Traffic and emission simulation in China based on statistical methodology. *Atmos Environ* 2011; **45**: 1154–61.
166. Cao G, Zhang X and Gong S *et al.* Emission inventories of primary particles and pollutant gases for China. *Chin Sci Bull* 2011; **56**: 781–8.
167. Li W, Fu L and Hao JM *et al.* Emission inventory of 10 kinds of air pollutants for road traffic vehicles in China (in Chinese). *Urban Env Urban Ecol* 2003; **16**: 36–8.
168. Liu JF, Zhao J and Li TT *et al.* Establishment of Chinese anthropogenic source volatile organic compounds emission inventory (in Chinese). *China Environ Sci* 2008; **28**: 496–500.
169. Wei W, Wang S and Hao J *et al.* Trends of chemical speciation profiles of anthropogenic volatile organic compounds emissions in China, 2005–2020. *Front Environ Sci Eng* 2014; **8**: 27–41.

Downloaded from https://academic.oup.com/nsr/article-abstract/4/6/834/4775139
by guest
on 14 February 2018

170. Song Y, Shao M and Liu Y *et al.* Source apportionment of ambient volatile organic compounds in Beijing. *Environ Sci Technol* 2007; **41**: 4348–53.
171. Wang S, Zhao M and Xing J *et al.* Quantifying the air pollutants emission reduction during the 2008 Olympic Games in Beijing. *Environ Sci Technol* 2010; **44**: 2490–6.
172. Wang M, Shao M and Chen W *et al.* Trends of non-methane hydrocarbons (NMHC) emissions in Beijing during 2002–2013. *Atmos Chem Phys* 2015; **15**: 1489–502.
173. Yamada H. Contribution of evaporative emissions from gasoline vehicles toward total VOC emissions in Japan. *Sci Total Environ* 2013; **449**: 143–9.
174. Liu H, Man H and Tschantz M *et al.* VOC from vehicular evaporation emissions: status and control strategy. *Environ Sci Technol* 2015; **49**: 14424–31.
175. Gee IL and Sollars CJ. Ambient air levels of volatile organic compounds in Latin American and Asian cities. *Chemosphere* 1998; **36**: 2497–506.
176. Na K and Kim YP. Seasonal characteristics of ambient volatile organic compounds in Seoul, Korea. *Atmos Environ* 2001; **35**: 2603–14.
177. Ho KF, Lee SC and Guo H *et al.* Seasonal and diurnal variations of volatile organic compounds (VOCs) in the atmosphere of Hong Kong. *Sci Total Environ* 2004; **322**: 155–66.
178. Ting M, Yue-si W and Hong-hui X *et al.* A study of the atmospheric VOCs of Mount Tai in June 2006. *Atmos Environ* 2009; **43**: 2503–8.
179. Liu Y, Shao M and Fu L *et al.* Source profiles of volatile organic compounds (VOCs) measured in China: Part I. *Atmos Environ* 2008; **42**: 6247–60.
180. Zhang Y, Wang X and Zhang Z *et al.* Species profiles and normalized reactivity of volatile organic compounds from gasoline evaporation in China. *Atmos Environ* 2013; **79**: 110–8.
181. Harley RA, Coulter-Burke SC and Yeung TS. Relating liquid fuel and headspace vapor composition for California reformulated gasoline samples containing ethanol. *Environ Sci Technol* 2000; **34**: 4088–94.
182. Hwa M-Y, Hsieh C-C and Wu T-C *et al.* Real-world vehicle emissions and VOCs profile in the Taipei tunnel located at Taiwan Taipei area. *Atmos Environ* 2002; **36**: 1993–2002.
183. Man H, Liu H and Niu H *et al.* VOC evaporative emissions from vehicles in China: Chemical characters and source apportionment (By personal communication).
184. Pang Y, Fuentes M and Rieger P. Trends in the emissions of Volatile Organic Compounds (VOCs) from light-duty gasoline vehicles tested on chassis dynamometers in Southern California. *Atmos Environ* 2014; **83**: 127–35.
185. Mellios G, Samaras Z and Martini G *et al.* A vehicle testing programme for calibration and validation of an evaporative emissions model. *Fuel* 2009; **88**: 1504–12.
186. U.S. Environmental Protection Agency (U.S. EPA). Development of Evaporative Emissions Calculations for the Motor Vehicle Emissions Simulator MOVES2010. 2012. Assessment and Standards Division, Office of Transportation and Air Quality, U.S. Environmental Protection Agency, EPA-420-R-12-027, available at https://nepis.epa.gov
187. Huang C, Wang HL and Li L *et al.* VOC species and emission inventory from vehicles and their SOA formation potentials estimation in Shanghai, China. *Atmos Chem Phys* 2015; **15**: 11081–96.
188. Dong X, Tschantz M and Fu JS. Estimating evaporative vapor generation from automobiles based on parking activities. *Environ Pollut* 2015; **202**: 104–11.
189. Yang X, Liu H and Cui H *et al.* Vehicular volatile organic compounds losses due to refueling and diurnal process in China: 2010–2050. *J Environ Sci* 2015; **33**: 88–96.
190. Mellios G and Samaras Z. An empirical model for estimating evaporative hydrocarbon emissions from canister-equipped vehicles. *Fuel* 2007; **86**: 2254–61.
191. Kean AJ, Sawyer RF and Harley RA. A fuel-based assessment of off-road diesel engine emissions. *JAPCA J Air Waste MA* 2000; **50**: 1929–39.
192. Wang F, Li Z and Zhang K *et al.* An overview of non-road equipment emissions in China. *Atmos Environ* 2016; **132**: 283–9.
193. United Nations Conference on Trade and Development. *Review of Maritime Transport 2016*, 2016.
194. Yang D-q, Kwan SH and Lu T *et al.* An emission inventory of marine vessels in Shanghai in 2003. *Environ Sci Technol* 2007; **41**: 5183–90.
195. Jin T-s, Yin X and Xu J *et al.* Air pollutants emission inventory from commercial ships of Tianjin Harbor (in Chinese). *Marine Environ Sci* 2009; **06**: 623–25.
196. Zhang L-j, Zheng J-y and Yin S-s *et al.* Development of non-road mobile source emission inventory for the Pearl River Delta region (in Chinese). *Environ Sci Technol* 2010; **31**: 886.
197. Fu Q, Shen Y and Zhang J. On the ship pollutant emission inventory in Shanghai port (in Chinese). *J Safety Environ* 2012; **05**: 57–64.
198. Ye S, Zheng J and Pan Y *et al.* Marine emission inventory and its temporal and spatial characteristics in Guangdong Province (in Chinese). *Acta Scientiae Circumstantiae* 2014; **34**: 537–47.
199. Li Z and He L. Emission inventory estimation methods study of ship pollutants (in Chinese). *Guangxi Journal of Light Industry* 2011; **27**: 79–80.
200. Zhang Y, Yang X and Brown R *et al.* Shipping emissions and their impacts on air quality in China. *Sci Total Environ* 2017; **581**: 186–98.
201. Liu H, Fu M and Jin X *et al.* Health and climate impacts of ocean-going vessels in East Asia. *Nat Clim Change* 2016; **6**: 1037–41.
202. Chen D, Wang X and Li Y *et al.* High-spatiotemporal-resolution ship emission inventory of China based on AIS data in 2014. *Sci Total Environ* 2017; **609**: 776–87.
203. Fu M, Liu H and Jin X *et al.* National- to port-level inventories of shipping emissions in China. *Environ Res Lett* 2017; **12**: 114024.
204. Fan Q, Zhang Y and Ma W *et al.* Spatial and seasonal dynamics of ship emissions over the Yangtze River Delta and East China Sea and their potential environmental influence. *Environ Sci Technol* 2016; **50**: 1322–9.
205. Li C, Yuan Z and Ou J *et al.* An AIS-based high-resolution ship emission inventory and its uncertainty in Pearl River Delta region, China. *Sci Total Environ* 2016; **573**: 1–10.
206. Mao X, Cui H and Roy B *et al.* Distribution of air pollution from oceangoing vessels in the Greater Pearl River Delta, 2015. *The International Council on Clean Transportation* 2017; **10**: 1–8.
207. International Maritime Organization (IMO). Second IMO GHG Study 2009, London, UK, 2009.
208. International Maritime Organization (IMO). Third IMO GHG Study 2014 Executive Summary and Final Report. London: International Maritime Organization, 2015.
209. Entec UK Limited. Quantification of Emissions from Ships Associated with Ship Movements between Ports in the European Community. 2002. Online available at: http://ec.europa.eu/environment/air/pdf/chapter1_ship_emissions.pdf.
210. European Environment Agency (EEA). The impact of international shipping on European air quality and climate forcing. Luxembourg: Publications Office of the European Union, 2013.

Downloaded from https://academic.oup.com/nsr/article-abstract/4/6/834/4775139
by guest
on 14 February 2018

211. U.S. Environmental Protection Agency (U.S. EPA). Proposal to Designate an Emission Control Area for Nitrogen Oxides, Sulfur Oxides and Particulate Matter. 2009. Online available at: https://www.epa.gov/sites/production/files/2016-09/documents/420r09007.pdf.
212. ICF International. Current Methodologies and Best Practices for Preparing Ocean Going Vessel Emission Inventories Used in Preparing the U.S. ECA Proposal for U.S.EPA. 2010. Online available at: https://www.epa.gov/sites/production/files/2014-05/documents/annexvi.pdf.
213. Fu M, Ding Y and Ge Y *et al.* Real-world emissions of inland ships on the Grand Canal, China. *Atmos Environ* 2013; **81**: 222–9.
214. Lou D, Shi L and Hu Z *et al.* Experimental study on emissions characteristics of inland ships based on different fuel qualities (in Chinese). *Ship Engineering* 2016; **07**: 49–53+7.
215. Peng Z, Ge Y and Tan J *et al.* Emissions from several in-use ships tested by portable emission measurement system. *Ocean Eng* 2016; **116**: 260–7.
216. Zhang F, Chen Y and Tian C *et al.* Emission factors for gaseous and particulate pollutants from offshore diesel engine vessels in China. *Atmos Chem Phys* 2016; **16**: 6319–34.
217. LMIS. The Lloyd's Maritime Database (CD-ROM). Ltd L s R F Editor. 2002.
218. Jalkanen JP, Johansson L and Kukkonen J. A comprehensive inventory of ship traffic exhaust emissions in the European sea areas in 2011. *Atmos Chem Phys* 2016; **16**: 71–84.
219. Yin P, Huang Z and Zheng D *et al.* Marine vessel emission and its temporal and spatial distribution characteristics in Ningbo-Zhoushan Port (in Chinese). *China Environ Sci* 2017; **37**: 27–37.
220. Song S. Ship emissions inventory, social cost and eco-efficiency in Shanghai Yangshan port. *Atmos Environ* 2014; **82**: 288–97.
221. Yao X, Mou J and Chen P *et al.* Ship emission inventories in estuary of the Yangtze River using terrestrial AIS data. *TransNav* 2016; **10**: 633–40.
222. Yang J, Yin P-l and Ye S-q *et al.* Marine emission inventory and its temporal and spatial characteristics in the city of Shenzhen. *Huan Jing Ke Xue* 2015; **36**: 1217–26.
223. Ng SKW, Loh C and Lin C *et al.* Policy change driven by an AIS-assisted marine emission inventory in Hong Kong and the Pearl River Delta. *Atmos Environ* 2013; **76**: 102–12.
224. Yau PS, Lee SC and Corbett JJ *et al.* Estimation of exhaust emission from ocean-going vessels in Hong Kong. *Sci Total Environ* 2012; **431**: 299–306.
225. Xing H, Duan S and Huang L *et al.* AIS data-based estimation of emissions from sea-going ships in Bohai Sea areas. *China Environ Sci* 2016; **36**: 953–60.
226. Song Y, Ge Y and Beijing Institute of Technology . Research of Emission Inventory and Emission Character of Inland and Offshore Ship. *Report for the Energy Foundation (in Chinese)* 2015.
227. Chen D, Zhao Y and Nelson P *et al.* Estimating ship emissions based on AIS data for port of Tianjin, China. *Atmos Environ* 2016; **145**: 10–18.
228. Chen D, Wang X and Nelson P *et al.* Ship emission inventory and its impact on the PM 2.5 air pollution in Qingdao Port, North China. *Atmos Environ* 2017; **166**: 351–61.
229. Liu J. The Establishment and application of ship emissions inventory in Qingdao Port (in Chinese). *Environmental Monitoring in China* 2011; **27**: 50–3.
230. Tan JW, Song YN and Ge YS *et al.* Emission inventory of ocean-going vessels in Dalian Coastal area. *Res Environ Sci* 2014; **12**: 1426–31.
231. Cullinane K, Tseng P-H and Wilmsmeier G. Estimation of container ship emissions at berth in Taiwan. *Int J Sustain Transp* 2016; **10**: 466–74.
232. Fan S and Nie L. Fuel consumption based exhaust emissions estimating from agricultural equipment in Beijing. *J Saf Environ* 2011; **11**: 145–8.
233. Fu M, Ding Y and Yin H *et al.* Characteristics of agricultural tractors emissions under real-world operating cycle. *Transactions of the Chinese Society of Agricultural Engineering* 2013; **29**: 42–8.
234. Ge Y, Liu H and Ding Y *et al.* Experimental study on characteristics of emissions and fuel consumption for combines. *Transactions of the Chinese Society of Agricultural Engineering* 2013; **29**: 41–7.
235. Li D-L, Wu Y and Zhou Y *et al.* Fuel consumption and emission inventory of typical construction equipments in China (in Chinese). *Huan Jing Ke Xue* 2012; **33**: 518–24.
236. Wu R and Xie S. Spatial distribution of ozone formation in China derived from emissions of speciated volatile organic compounds. *Environ Sci Technol* 2017; **51**: 2574–83.
237. Zhao Y, Mao P and Zhou Y *et al.* Improved provincial emission inventory and speciation profiles of anthropogenic non-methane volatile organic compounds: a case study for Jiangsu, China. *Atmos Chem Phys* 2017; **17**: 7733–56.
238. Huang X, Song Y and Li M *et al.* A high-resolution ammonia emission inventory in China. *Global Biogeochem Cycles* 2012; **26**: GB1030.
239. Gu B, Ju X and Chang J *et al.* Integrated reactive nitrogen budgets and future trends in China. *Proc Natl Acad Sci USA* 2015; **112**: 8792–7.
240. Kang Y, Liu M and Song Y *et al.* High-resolution ammonia emissions inventories in China from 1980 to 2012. *Atmos Chem Phys* 2016; **16**: 2043–58.
241. Huo Q, Cai X and Kang L *et al.* Estimating ammonia emissions from a winter wheat cropland in North China Plain with field experiments and inverse dispersion modeling. *Atmos Environ* 2015; **104**: 1–10.
242. Van Damme M, Clarisse L and Heald CL *et al.* Global distributions, time series and error characterization of atmospheric ammonia (NH_3) from IASI satellite observations. *Atmos Chem Phys* 2014; **14**: 2905–22.
243. Warner JX, Dickerson RR and Wei Z *et al.* Increased atmospheric ammonia over the world's major agricultural areas detected from space. *Geophys Res Lett* 2017; **44**: 2875–84.
244. Paulot F, Jacob DJ and Pinder RW *et al.* Ammonia emissions in the United States, European Union, and China derived by high-resolution inversion of ammonium wet deposition data: Interpretation with a new agricultural emissions inventory (MASAGE˙NH3). *J Geophy Res Atmos* 2014; **119**: 4343–64.
245. Streets DG, Yarber KF and Woo JH *et al.* Biomass burning in Asia: annual and seasonal estimates and atmospheric emissions. *Global Biogeochem Cycles* 2003; **17**: 1099.
246. Song Y, Liu B and Miao W *et al.* Spatiotemporal variation in nonagricultural open fire emissions in China from 2000 to 2007. *Global Biogeochem Cycles* 2009; **23**: GB2008.
247. Randerson JT, Chen Y and van der Werf GR *et al.* Global burned area and biomass burning emissions from small fires. *J Geophys Res* 2012; **117**: G04012.
248. Wooster MJ. Small-scale experimental testing of fire radiative energy for quantifying mass combusted in natural vegetation fires. *Geophys Res Lett* 2002; **29**: 23-1–4.
249. Wooster MJ, Roberts G and Perry GLW *et al.* Retrieval of biomass combustion rates and totals from fire radiative power observations: FRP derivation and calibration relationships between biomass consumption and fire radiative energy release. *J Geophys Res* 2005; **110**: D24311.
250. Vermote E, Ellicott E and Dubovik O *et al.* An approach to estimate global biomass burning emissions of organic and black carbon from MODIS fire radiative power. *J Geophys Res* 2009; **114**: D18205.
251. Kaiser JW, Heil A and Andreae MO *et al.* Biomass burning emissions estimated with a global fire assimilation system based on observed fire radiative power. *Biogeosciences* 2012; **9**: 527–54.

Downloaded from https://academic.oup.com/nsr/article-abstract/4/6/834/4775139
by guest
on 14 February 2018

252. Liu M, Song Y and Yao H *et al.* Estimating emissions from agricultural fires in the North China Plain based on MODIS fire radiative power. *Atmos Environ* 2015; **112**: 326–34.
253. Xu W, Wooster MJ and Kaneko T *et al.* Major advances in geostationary fire radiative power (FRP) retrieval over Asia and Australia stemming from use of Himarawi-8 AHI. *Remote Sens Environ* 2017; **193**: 138–49.
254. Saikawa E, Kim H and Zhong M *et al.* Comparison of emissions inventories of anthropogenic air pollutants and greenhouse gases in China. *Atmos Chem Phys* 2017; **17**: 6393–421.
255. Xia Y, Zhao Y and Nielsen CP. Benefits of China's efforts in gaseous pollutant control indicated by the bottom-up emissions and satellite observations 2000–2014 *Atmos Environ* 2016; **136**: 43–53.
256. van Donkelaar A, Martin RV and Leaitch WR *et al.* Analysis of aircraft and satellite measurements from the Intercontinental Chemical Transport Experiment (INTEX-B) to quantify long-range transport of East Asian sulfur to Canada. *Atmos Chem Phys* 2008; **8**: 2999–3014.
257. Yan H, Chen L and Su L *et al.* SO2 columns over China: temporal and spatial variations using OMI and GOME-2 observations. *IOP C Ser Earth Env* 2014; **17**: 012027.
258. Krotkov NA, McLinden CA and Li C *et al.* Aura OMI observations of regional SO_2 and NO_2 pollution changes from 2005 to 2015. *Atmos Chem Phys* 2016; **16**: 4605–29.
259. van der A RJ, Mijling B and Ding J *et al.* Cleaning up the air: effectiveness of air quality policy for SO_2 and NO_x emissions in China. *Atmos Chem Phys* 2017; **17**: 1775–89.
260. Shi Y, Xia Y-f and Lu B-h *et al.* Emission inventory and trends of NO_x for China, 2000–2020. *J Zheijang Univ-Sci* 2014; **15**: 454–64.
261. Richter A, Burrows JP and Nusz H *et al.* Increase in tropospheric nitrogen dioxide over China observed from space. *Nature* 2005; **437**: 129–32.
262. Berezin EV, Konovalov IB and Ciais P *et al.* Multiannual changes of CO_2 emissions in China: indirect estimates derived from satellite measurements of tropospheric NO_2 columns. *Atmos Chem Phys* 2013; **13**: 9415–38.
263. Gu D, Wang Y and Smeltzer C *et al.* Reduction in NO_x emission trends over China: regional and seasonal variations. *Environ Sci Technol* 2013; **22**: 12912–9.
264. Mijling B, van der A RJ and Zhang Q. Regional nitrogen oxides emission trends in East Asia observed from space. *Atmos Chem Phys* 2013; **13**: 12003–12.
265. Itahashi S, Uno I and Irie H *et al.* Regional modeling of tropospheric NO_2 vertical column density over East Asia during the period 2000–2010: comparison with multisatellite observations. *Atmos Chem Phys* 2014; **14**: 3623–35.
266. Miyazaki K, Eskes H and Sudo K *et al.* Decadal changes in global surface NO_x emissions from multi-constituent satellite data assimilation. *Atmos Chem Phys* 2017; **17**: 807–37.
267. Liu F, Zhang Q and Ronald JvdA *et al.* Recent reduction in NO_x emissions over China: synthesis of satellite observations and emission inventories. *Environ Res Lett* 2016; **11**: 114002.
268. Streets DG, Zhang Q and Wang L *et al.* Revisiting China's CO emissions after the Transport and Chemical Evolution over the Pacific (TRACE-P) mission: synthesis of inventories, atmospheric modeling, and observations. *J Geophys Res* 2006; **111**: D14306.
269. Worden HM, Deeter MN and Frankenberg C *et al.* Decadal record of satellite carbon monoxide observations. *Atmos Chem Phys* 2013; **13**: 837–50.
270. Yumimoto K, Uno I and Itahashi S. Long-term inverse modeling of Chinese CO emission from satellite observations. *Environ Pollut* 2014; **195**: 308–18.
271. Yin Y, Chevallier F and Ciais P *et al.* Decadal trends in global CO emissions as seen by MOPITT. *Atmos Chem Phys* 2015; **15**: 13433–51.
272. Streets DG, Hao J and Wu Y *et al.* Anthropogenic mercury emissions in China. *Atmos Environ* 2005; **39**: 7789–806.
273. Streets DG, Devane MK and Lu Z *et al.* All-time releases of mercury to the atmosphere from human activities. *Environ Sci Technol* 2011; **45**: 10485–91.
274. Wu QR, Wang SX and Zhang L *et al.* Update of mercury emissions from China's primary zinc, lead and copper smelters, 2000–2010. *Atmos Chem Phys* 2012; **12**: 11153–63.
275. Chen Y, Wang R and Shen H *et al.* Global mercury emissions from combustion in light of international fuel trading. *Environ Sci Technol* 2014; **48**: 1727–35.
276. Tian H, Zhu CY and Gao JJ *et al.* Quantitative assessment of atmospheric emissions of toxic heavy metals from anthropogenic sources in China: historical trend, spatial distribution, uncertainties, and control policies. *Atmos Chem Phys* 2015; **15**: 10127–47.
277. Smith SJ, van Aardenne J and Klimont Z *et al.* Anthropogenic sulfur dioxide emissions: 1850–2005. *Atmos Chem Phys* 2011; **11**: 1101–16.
278. Li J, Li LY and Wu RR *et al.* Inventory of highly resolved temporal and spatial volatile organic compounds emission in China. In: *24th International Conference on Modelling, Monitoring and Management of Air Pollution (AIR 2016), 2016*. Abstract Air Pollution XXIV. WIT Transactions on Ecology and The Environment.
279. Cao G, Zhang X and Zheng F. Inventory of black carbon and organic carbon emissions from China. *Atmos Environ* 2006; **40**: 6516–27.
280. Qin Y and Xie SD. Spatial and temporal variation of anthropogenic black carbon emissions in China for the period 1980–2009. *Atmos Chem Phys* 2012; **12**: 4825–41.
281. Dong W, Xing J and Wang S. Temporal and spatial distribution of anthropogenic ammonia emissions in China: 1994–2006. *Environ Sci* 2010; **31**: 1457–63.
282. Gu B, Ge Y and Ren Y *et al.* Atmospheric reactive nitrogen in China: sources, recent trends, and damage costs. *Environ Sci Technol* 2012; **46**: 9420–7.
283. Xu P, Zhang Y and Gong W *et al.* An inventory of the emission of ammonia from agricultural fertilizer application in China for 2010 and its high-resolution spatial distribution. *Atmos Environ* 2015; **115**: 141–8.
284. Geng G, Zhang Q and Martin RV *et al.* Impact of spatial proxies on the representation of bottom-up emission inventories: a satellite-based analysis. *Atmos Chem Phys* 2017; **17**: 4131–45.
285. Zheng B, Zhang Q and Tong D *et al.* Resolution dependence of uncertainties in gridded emission inventories: a case study in Hebei, China. *Atmos Chem Phys* 2017; **17**: 921–33.
286. Zhou Y, Zhao Y and Mao P *et al.* Development of a high-resolution emission inventory and its evaluation and application through air quality modeling for Jiangsu Province, China. *Atmos Chem Phys* 2017; **17**: 211–33.
287. Wang SS, Zheng J and Fu F *et al.* Development of an emission processing system for the Pearl River Delta Regional air quality modeling using the SMOKE model: methodology and evaluation. *Atmos Environ* 2011; **45**: 5079–89.
288. Woo J-H, Choi K-C and Kim HK *et al.* Development of an anthropogenic emissions processing system for Asia using SMOKE. *Atmos Environ* 2012; **58**: 5–13.
289. Chen H, Huang Y and Shen H *et al.* Modeling temporal variations in global residential energy consumption and pollutant emissions. *Appl Energ* 2016; **184**: 820–9.

Downloaded from https://academic.oup.com/nsr/article-abstract/4/6/834/4775139
by guest
on 14 February 2018

290. Zheng J, Zhang L and Che W *et al.* A highly resolved temporal and spatial air pollutant emission inventory for the Pearl River Delta region, China and its uncertainty assessment. *Atmos Environ* 2009; **43**: 5112–22.
291. Carter WPL. *Documentation of the SAPRC-99 Chemical Mechanism for VOC Reactivity Assessment, Report to the California Air Resources Board*. CA: University of California, Riverside, USA, 2000.
292. Carter WPL. Development of the SAPRC-07 chemical mechanism. *Atmos Environ* 2010; **44**: 5324–35.
293. Gery MW, Whitten GZ and Killus JP *et al.* A photochemical kinetics mechanism for urban and regional scale computer modeling. *J Geophys Res* 1989; **94**: 12925–56.
294. Zaveri RA and Peters LK. A new lumped structure photochemical mechanism for large-scale applications. *J Geophys Res* 1999; **104**: 30387–415.
295. Yarwood G, Rao S and Yocke M *et al.* Updates to the carbon bond chemical mechanism: CB05, *Final Report to the US EPA, RT-0400675,* Novato, CA, 2005. Online available at: http://www.camx.com/files/cb05_final_report_120805.aspx
296. Stockwell WR, Middleton P and Chang JS *et al.* The second generation regional acid deposition model chemical mechanism for regional air quality modeling. *J Geophys Res* 1990; **95**: 16343–67.
297. Stockwell WR, Kirchner F and Kuhn M *et al.* A new mechanism for regional atmospheric chemistry modeling. *J Geophys Res* 1997; **102**: 25847–79.
298. Goliff WS, Stockwell WR and Lawson CV. The regional atmospheric chemistry mechanism, version 2. *Atmos Environ* 2013; **68**: 174–85.
299. Mo Z, Shao M and Lu S. Compilation of a source profile database for hydrocarbon and OVOC emissions in China. *Atmos Environ* 2016; **143**: 209–17.
300. Yuan B, Shao M and Lu S *et al.* Source profiles of volatile organic compounds associated with solvent use in Beijing, China. *Atmos Environ* 2010; **44**: 1919–26.
301. Wang H, Qiao Y and Chen C *et al.* Source profiles and chemical reactivity of volatile organic compounds from solvent use in Shanghai, China. *Aerosol Air Qual Res* 2014; **14**: 301–10.
302. Zheng J, Yu Y and Mo Z *et al.* Industrial sector-based volatile organic compound (VOC) source profiles measured in manufacturing facilities in the Pearl River Delta, China. *Sci Total Environ* 2013; **456**: 127–36.
303. Wei W, Cheng S and Li G *et al.* Characteristics of ozone and ozone precursors (VOCs and NOx) around a petroleum refinery in Beijing, China. *J Environ Sci* 2014; **26**: 332–42.
304. Mo Z, Shao M and Lu S *et al.* Process-specific emission characteristics of volatile organic compounds (VOCs) from petrochemical facilities in the Yangtze River Delta, China. *Sci Total Environ* 2015; **533**: 422–31.
305. He Q. Preliminary study on profiles of VOC˙S emitted from coking (in Chinese). *Environmental Monitoring in China* 2005; **21**: 61–5.
306. Tsai WY, Chan LY and Blake DR *et al.* Vehicular fuel composition and atmospheric emissions in South China: Hong Kong, Macau, Guangzhou, and Zhuhai. *Atmos Chem Phys* 2006; **6**: 3281–8.
307. Wang J, Jin L and Gao J *et al.* Investigation of speciated VOC in gasoline vehicular exhaust under ECE and EUDC test cycles. *Sci Total Environ* 2013; **445**: 110–6.
308. Dong D, Shao M and Li Y *et al.* Carbonyl emissions from heavy-duty diesel vehicle exhaust in China and the contribution to ozone formation potential. *J Environ Sci* 2014; **26**: 122–8.
309. Ou J, Feng X and Liu Y *et al.* Source characteristics of VOCs emissions from vehicular exhaust in the Pearl River Delta region. *Acta Scientiae Circumstantiae* 2014; **34**: 827–34.
310. Yao Z, Shen X and Ye Y *et al.* On-road emission characteristics of VOCs from diesel trucks in Beijing, China. *Atmos Environ* 2015; **103**: 87–93.
311. Yao Z, Wu B and Shen X *et al.* On-road emission characteristics of VOCs from rural vehicles and their ozone formation potential in Beijing, China. *Atmos Environ* 2015; **105**: 91–6.
312. Cao X, Yao Z and Shen X *et al.* On-road emission characteristics of VOCs from light-duty gasoline vehicles in Beijing, China. *Atmos Environ* 2016; **124**: 146–55.
313. Yue T, Yue X and Chai F *et al.* Characteristics of volatile organic compounds (VOCs) from the evaporative emissions of modern passenger cars. *Atmos Environ* 2017; **151**: 62–9.
314. Ou J, Zheng J and Li R *et al.* Speciated OVOC and VOC emission inventories and their implications for reactivity-based ozone control strategy in the Pearl River Delta region, China. *Sci Total Environ* 2015; 530–1: 393–402.
315. Appel KW, Napelenok SL and Foley KM *et al.* Description and evaluation of the Community Multiscale Air Quality (CMAQ) modeling system version 5.1. *Geosci Model Dev* 2017; **10**: 1703–32.
316. Reff A, Bhave PV and Simon H *et al.* Emissions inventory of PM2.5 trace elements across the United States. *Environ Sci Technol* 2009; **43**: 5790–6.
317. Yi HH. Studies on emission characteristics of PM10 from power plants. *Ph.D. Thesis*. Tsinghua University 2006.
318. Wang W. Studies on emissions characteristics of PM for typical stationary combustion source. *Master's Thesis*. Chinese Research Academy of Environmental Sciences 2007.
319. Pei B, Wang X and Zhang Y *et al.* Emissions and source profiles of PM2.5 for coal-fired boilers in the Shanghai megacity, China. *Atmos Pollut Res* 2016; **7**: 577–84.
320. Li C, Li X-H and Duan L *et al.* Emission characteristics of PM10 from coal-fired industrial boiler. *Huan Jing Ke Xue* 2009; **30**: 650–5.
321. Li X, Wang S and Duan L *et al.* Particulate and trace gas emissions from open burning of wheat straw and corn stover in China. *Environ Sci Technol* 2007; **41**: 6052–8.
322. He L-Y, Hu M and Zhang Y-H *et al.* Fine particle emissions from on-road vehicles in the Zhujiang Tunnel, China. *Environ Sci Technol* 2008; **42**: 4461–6.
323. Cheng Y, Lee SC and Ho KF *et al.* Chemically-speciated on-road PM2.5 motor vehicle emission factors in Hong Kong. *Sci Total Environ* 2010; **408**: 1621–7.
324. Ma JY. Research on emission characteristics of air pollutants from cement industry. *Master's Thesis*. Hebei University of Engineering 2010.
325. Ma JH. Emission characteristics of particulates from typical production process of iron and steel enterprises. *Master's Thesis*. Southwest University 2009.
326. Li CQ. Characterization of air pollutants emitted from coking production. *Master's Thesis*. Southwest University 2009.
327. Zhao Y, Nielsen CP and McElroy MB *et al.* CO emissions in China: uncertainties and implications of improved energy efficiency and emission control. *Atmos Environ* 2012; **49**: 103–13.
328. Zhao Y, Qiu LP and Xu RY *et al.* Advantages of a city-scale emission inventory for urban air quality research and policy: the case of Nanjing, a typical industrial city in the Yangtze River Delta, China. *Atmos Chem Phys* 2015; **15**: 12623–44.

Downloaded from https://academic.oup.com/nsr/article-abstract/4/6/834/4775139
by guest
on 14 February 2018